

240

FINAL REPORT

PARTICIPATION IN THE APOLLO PASSIVE SEISMIC
EXPERIMENT

NASA Contract NGR 22-009-123

Prepared by

Frank Press, M. Nafi Toksöz

and

Anton Dainty

(NASA-CR-137239) PARTICIPATION IN THE
APOLLO PASSIVE SEISMIC EXPERIMENT Final
Report (Massachusetts Inst. of Tech.)
67 p HC \$6.50

CSCI 03B

74-19499

G3/30

Unclas
32693

3 July 1972

Department of Earth and Planetary Sciences

Massachusetts Institute of Technology

Cambridge, Massachusetts 02139

ABSTRACT

Under this contract, computer programs were written to read digital tapes prepared at MSC, Houston, containing the data, and to interpret the resulting information. The MIT group concentrated on two aspects of this interpretation as follows. Using the very early parts of the lunar seismogram and interpreting these parts as seismic body-wave phases enabled a determination to be made of the structure of the outer part of the moon in the Fra Mauro region using the impacts of the S-IV-B Booster and LM Ascent stage from the various missions. This study shows that the moon has a crust in the Fra Mauro region 60 to 65 km-thick overlaying a high velocity mantle. The crust is further divided into an upper part, 25 km thick, apparently made of material similar to the surficial basalts, and a lower part of seemingly different composition, possibly an anorthositic gabbro. The second area studied under this contract has been the generation of the exceedingly long reverberating wave-train observed in lunar seismogram. This is believed to be due to an intensely scattering layer with very high quality coefficient $Q(\sim 4,000)$ overlying a more homogeneous elastic medium. In addition to these major areas, the MIT group assisted other groups in the Passive Seismic Experiment team with other phases of the investigation.

CONTENTS

	Page
ABSTRACT	i
CHAPTER 1	
Introduction	1
CHAPTER 2	
Structure, Composition and Properties of Lunar Crust	3
CHAPTER 3	
Seismic Scattering in the Moon and the Earth	42
APPENDIX A	
Titles and Abstracts of Published Papers (Supported by Contract)	55
APPENDIX B	
List of Oral Presentations	63

CHAPTER 1 - INTRODUCTION

The Apollo Passive Seismic Experiment produces more data than any other experiment in the Alsep package. Three components of ground displacement are measured at a rate of about five samples a second each by the long-period seismometer (hereinafter, this instrument will be abbreviated as LP; LPZ, for example, will refer to the vertical component of ground motion measured by it); in addition, there are tidal outputs from this instrument for each component once every two seconds. Simultaneously, the short-period seismometer (SPZ) is measuring the vertical component of ground displacement at a rate of about 50 per second. Data is transmitted to earth continuously, 24 hours a day, and during the latter part of the contract, three stations (Apollo Missions 12, 14 and 15) were operating simultaneously.

To handle the enormous amount of data generated, different groups in the Passive Seismic Experiment Team, under the direction of Professor Gary Latham of Lamont Geological Observatory, undertook different tasks. Only the Lamont group, working under NASA contracts NAS9-5957 and NAS9-5632, has made a preliminary examination of all the data; it was not feasible for the MIT group to do so with the computer facilities available to them. The MIT group has instead concentrated on two areas of study--

the interpretation of lunar structure using very early portions of the lunar seismograms from artificial impacts (Chapter 2), and an analysis of seismic scattering in the moon (Chapter 3). These areas were chosen as particularly appropriate to MIT's combination of expertise, manpower, and computer facilities. In addition, the MIT group provided inputs of advice, information, and expertise to other groups in the Passive Seismic Experiment Team engaged in studies of other areas (such as moonquakes and meteorite impacts)--and received inputs from other groups in their own areas. Also, the MIT group was available for support during missions. Appendix A contains the titles and abstracts of papers published under this contract, and Appendix B contains a list of oral presentations.

As can be seen, this study required considerable computation. The facilities available at MIT were an IBM 360/370 central processor, and a time-sharing system, Multics. The data was supplied on tapes from the Manned Spacecraft Center, Houston. Programs were written to read these tapes, display the data, bandpass filter it, rotate the coordinate system to any desired azimuth, and perform other useful operations on the data, such as deglitching. A large repertoire of computational techniques for interpretation of seismic data is available at MIT, and full use was made of it. In addition, programs for interpretation of data were written as necessary.

Chapter 2

STRUCTURE, COMPOSITION, AND PROPERTIES OF LUNAR CRUST

by

M. N. Toksöz, F. Press, A. Dainty, and K. Anderson

Department of Earth and Planetary Sciences

Massachusetts Institute of Technology

INTRODUCTION

WITH THE SUCCESSFUL recording of Lunar Module (LM) ascent stage and Saturn (S-IV B) rocket impacts by the Apollo 12, 14 and 15 seismometers, discrete seismic phases which can be interpreted in terms of a velocity structure inside the moon have become available. Travel times, amplitudes, and wave shapes of compressional (P) and shear (S) waves have been obtained for distances between $\Delta = 67$ km and $\Delta = 357$ km. These data are inverted to determine the seismic velocity structures in the outer 100 km of the lunar interior. In this paper we describe the data, the inversion techniques, velocity models, compositional implications and the properties of the lunar interior in the light of laboratory measurements of velocities of lunar and terrestrial rocks. The data and the interpretation are more expansive than those of the two previous reports (TOKSÖZ et al., 1972a,b).

In the study of the earth's interior data from a large number of earthquakes of all magnitudes, numerous artificial sources (e.g., underground nuclear explosions) and more than a thousand seismic stations are being utilized. In the case of the moon the natural seismicity (both the number and energy of moonquakes) is many orders of magnitude lower than that of

the earth (LATHAM et al., 1971, 1972). With only three stations it is not possible at this stage to specify the epicenter coordinates, focal depth, and origin time of these events with sufficient accuracy to use them in structural studies. It has not been possible to detect long-period surface waves or free oscillations of the moon from such very small moonquakes. Thus we must rely on seismic waves from six artificial impacts, as recorded by the Apollo 12, 14 and 15 seismometers, for the study of the lunar interior.

SEISMIC DATA AND VELOCITY MODELS

Compressional and shear velocity profiles were obtained by interpreting the travel times and amplitudes of P and S waves recorded by the Passive Seismic Experiment (PSE) instruments. The locations of the three operating stations, impact points and wave paths are shown in Fig. 1; the distances are listed in Table 1. The general characteristics of all impact signals are very similar to each other. They are extremely prolonged with gradual build-up of the signal and very long exponential decay of signal intensity. Typically, duration of the signals is about two hours. These characteristics, which are believed to be caused by intensive scattering,

have been discussed previously (LATHAM et al., 1971; NAKAMURA et al., 1970; DAINTY and ANDERSON, 1972) and will not be treated here. The signals corresponding to the arrival of discrete seismic phases can be identified in the early parts of the records. These are of most interest for our study.

The initial portions of the impact seismograms are shown in Fig. 2. In order to understand this figure, it is important to keep in mind that the S-IV B impact precedes the lunar landing and thus is recorded by stations operating prior to the landing. The LM-ascent stage impact which occurs after the lunar landed mission is completed can be recorded with the instrument of the same mission. Furthermore, the kinetic energy of a typical S-IV B impact is about 13 times larger than that of a typical LM impact (see Table 1). The larger amplitudes of S-IV B impact signals relative to those of LM impacts are clear. The change in the signal characteristics from one record to another, at different distances such as $\Delta = 135, 172, \text{ and } 357 \text{ km}$, is also observed.

The travel times of seismic arrivals provide the most direct means of looking at the lunar interior. For P-waves times are read from high-pass filtered or unfiltered traces. Positive identification of the signal is made by the linear polarization of the particle motion. Shear wave phases have been tentatively identified on the records; primarily low-pass

filtered seismograms are used. As with P-waves, an attempt was made to use particle motion to identify S phases, but this did not always succeed. Many of the arrivals were identified on the transverse (T) traces (Fig. 3). Theoretically one would expect the S-waves to be generated less efficiently by the impacts than by the moonquakes. This is observed in the case of the lunar data analyzed. The S-wave amplitudes are generally small in the S-IV B and LM impact records as well as the records of natural meteoroid impacts. The S-wave travel times are not as accurate as those of P-waves. As a result of this, conclusions drawn concerning S-wave velocities should be treated with caution. The travel time-distance curves shown in Figs. 4 and 5 are composites of data for direct arrival P and S waves and later phases (surface-reflected PP, PPP, SS, SSS). Since both source and receiver are at the surface of the moon, for phases such as PP and SS the times can be plotted at equivalent distances for direct arrivals. The overall characteristics of the travel times indicate rapidly increasing velocities near the surface. An intermediate zone with nearly constant velocity and below this a high velocity zone are indicated by the two branches of the travel time curve between distances of 186 km and 357 km. In addition to these, later arrivals observed at 186 and 357 km indicate the presence of very high velocity gradients or

discontinuities inside the moon.

The amplitudes (Figs. 4, 5) provide further evidence for velocity discontinuities. Because the geometric focusing, defocusing and reflection of seismic rays are controlled by the velocity gradients (see ray paths in Fig. 4), the amplitudes are very sensitive indicators of rapid velocity variations. The amplitude data come from both the LM and S-IV B impact records. Since the sources have different energies, the amplitudes need to be scaled. We chose an empirical approach for this purpose and required a smooth transition from LM signal amplitudes to S-IV B signal amplitudes as a function of distance. This required a correction (multiplication) factor of 20 for LM amplitudes, a value larger than the square root of energy ratios. However, since the angles of impact (about 3° from horizontal for LM vs 62° or greater for S-IV B) and sizes of the impacting objects were different, it is reasonable that S-IV B impacts would be more efficient generators of seismic waves at frequencies below 1 Hz. The agreement between theoretical curves and observed amplitude and travel-time data is very good both for P- and S-waves.

A more definitive approach to interpreting the observed lunar seismograms is to compute their theoretical equivalents (HELMBERGER, 1968; HELMBERGER and WIGGINS, 1971). This requires, in addition to the velocity structure inside the moon,

knowledge of the seismic source pulse due to the impact and the exact impulse response of the seismometer emplaced at the surface on a very low-velocity regolith complex. To isolate the effect of the velocity structure, one must keep the other variables fixed. We chose the three S-IV B impact seismograms recorded by the Apollo 12 station. This had the advantage of keeping the instrument response fixed while the source-receiver distance increased for three nearly identical impacts. Because of the low signal-to-noise ratios, LM impact seismograms were excluded from matching.

The observed and computed seismograms at distances of $\Delta = 135, 172, \text{ and } 357$ km are shown in Fig. 6. The source function was chosen such that at 172 km the seismograms were matched exactly for the first 8 seconds. The general characteristics of the observed seismograms change significantly from $\Delta = 135$ km to 172 km and again from $\Delta = 172$ km to 357 km. These are matched very closely by the theoretical seismograms. Only P arrivals are matched in Fig. 6.

The S-wave data were interpreted using travel-time analysis and ray theory amplitudes. Since scattering was obviously important (as evidenced by the presence of transverse motion), synthetic seismograms were not computed. Amplitudes were measured on the radial component, unfiltered, even if the arrival was originally identified on the low-pass filter transverse

trace. Fig. 5 shows the fit of travel-times and measured amplitudes to the theoretical values for the S-velocity model shown in Fig. 7. This model was constrained to follow the P-velocity model, insofar as this was possible.

The velocity models finalized on the basis of the fit to the travel-times, amplitudes and synthetic seismograms are shown in Fig. 7. These models provide direct evidence for the presence of a layered lower crust. The main features of the velocity profiles are:

- i) Very rapid increase at shallow depths from the surface to 10 km depth. The details of the models and whether the velocities increase smoothly or step-wise in the upper 5 km cannot be resolved without additional data at distances closer than 30 km.
- ii) A sharp increase ("discontinuity") at a depth of about 25 km.
- iii) Near constant values between 25 and 65 km.
- iv) A significant and discontinuous increase at the base of the lunar crust (65 km).
- v) As can be determined from a single data point corresponding to the distance of 357 km, very high apparent velocities below the lunar crust.

From comparisons with velocities of the earth's crust and mantle, it is appropriate to define the base of the "lunar

crust" at the discontinuity at 65 km. Although this is greater than the average thickness of the earth's crust, the jump of the P velocity at this interface from about 7.0 to 9.0 km/sec is very similar to the increase at the Mohorovicic discontinuity. If hydrostatic pressure instead of depth is used as the variable, the base of the lunar crust occurs at a pressure of 3.5 kbars, which is reached at a depth of 10 km inside the earth.

COMPOSITION AND PROPERTIES

The compositional implications of the lunar velocity models can be explored with the aid of high-pressure laboratory measurements on lunar and terrestrial rocks. Velocity measurements have been made on lunar soils, breccias, and igneous rocks from four Apollo missions (ANDERSON et al., 1970; KANAMORI et al., 1970, 1971; WANG et al., 1971; WARREN et al., 1971, 1972; MIZUTANI et al., 1972; TITTMAN et al., 1972; TODD et al., 1972). Regardless of composition, these rocks are characterized by very low velocities at low pressures relative to terrestrial rocks. This can be attributed to the absence of water in the lunar rocks combined with the effects of porosity and micro-cracks. Laboratory measurements on

terrestrial igneous rocks have demonstrated this effect. As shown in Fig. 8 taken from NUR and SIMMONS (1969), with only 0.7% porosity, the velocity of compressional waves at pressures less than 0.5 kb is much lower in the dry state than in the saturated state. In dry-state conditions appropriate for the moon, the pressure gradient of compressional velocity is very high at low pressures, a behavior very similar to that of the lunar P velocity profile.

The measured velocities of lunar samples are plotted together with observed compressional and shear wave velocity profiles in Figs. 9 and 10 respectively. These figures show all available lunar rock velocities except the values for porphyritic basalts 12002 and 12022 (WANG et al., 1971). These two rocks have higher velocities than those of all other lunar rocks (about 0.6 km/sec higher than those of Apollo 11 and 14 basalts at 3 kb pressure). At the present the significance of this deviation is being investigated. Compressional velocities of terrestrial rocks shown in Fig. 9 represent either an average value for one or more measurements, or specify general bounds between which most values fall (see ANDERSON and LIEBERMAN, 1966; PRESS, 1966 for tabulations). The Poisson ratio σ [$\sigma = (V_p^2 - 2V_s^2)/2(V_p^2 + V_s^2)$], where V_p and V_s are velocities], shown in Fig 10b, is a strong indication of the rock conditions in the lunar crust.

To a depth of 25 km σ calculated from observed velocities falls among the lunar sample values and close to terrestrial dry granite. At greater depths, both the model values and Poisson's ratios of lunar samples increase, indicating the closing of microcracks. All lunar basalts (except for sample 10020) have higher Poisson's ratios than the observed value below about 30 km depth.

From the comparison of the laboratory data and the lunar velocity profile, the following units can be identified:

i) Near the surface the extremely low seismic velocities are very similar to those of lunar fines (soils) and broken rocks. The velocity increases very rapidly as a result of self-compaction under pressure. The exact depth to the bottom of the lunar regolith and the brecciated and fractured layer cannot be determined without additional travel-time data in the distance range of 0.1 to 5.0 km.

ii) Below a depth of a few kilometers the measured velocities of lunar basaltic rocks fit both the compressional and shear velocity profiles to a depth of about 25 km. The rapid increase of velocity to a depth of about 10 km can be explained by the pressure effect on dry rocks having micro- and macro-cracks. The observed velocity models seem to fall between the measured values for lunar basaltic rocks; Nos. 10057 and 12065, paralleling these curves to a depth of 25 km. They coincide with laboratory velocities of lunar samples 14310 and 10020. Whether this layer consists of a series of flows

or fairly thick intrusive basalt cannot be resolved with our data. Nor is it possible to rule out other compositions or rock types which may have similar velocities under a lunar environment.

There are other data indicating similar values for thicknesses of mare basalts. A model proposed by WOOD (1970) on the basis of density contrast and relative elevations of basaltic mare and "anorthositic" highlands, requires 25 km of basalt in the mare for isostatic compensation to occur. The latest gravity data from Apollo 15 subsatellite observations fits a model of about 20 km of basalt filling in mascon basins (SJOGREN et al., 1972).

iii) The second layer of the lunar crust (25 km to 65 km) appears to be made of competent rock. The increase in pressure affects velocities very little (velocity at the bottom is about 7.0 km/sec). The petrological interpretation of the velocity curve is not very simple. It is clear from Figs. 9 and 10 that available lunar sample velocities are lower than the observed curve if we exclude the two anomalous rocks 12002 and 12022. A rock of special interest is 15418, a recrystallized or annealed gabbroic anorthosite (LSPET, 1972). Laboratory values of velocities of 15418 are higher than other lunar values plotted in Figs. 9 and 10. However, they are still lower than the observed values below a depth of 25 km. We compared the laboratory data on terrestrial rocks to observed lunar velocity curves. The examples plotted on Figs. 9 and

10 represent some possible candidates. The observed P and S velocity curves fall in the middle of the laboratory data for gabbros. It is very close to the anorthosite values. The lower bound for terrestrial pyroxenite is slightly higher than the observed P curve. Eclogite and dunite velocities are definitely higher than the observations, and these cannot be considered as serious contenders.

Petrological evidence as well as velocities favor a composition of anorthositic gabbro or gabbroic anorthosite (WOOD et al., 1971; GAST and MCCONNELL, JR., 1972; REID et al., 1972; WALKER et al., 1972). However, the above evidence cannot rule out other interpretations.

iv) The discontinuity at 65 km depth is required to satisfy the amplitudes, travel-times, and most clearly the seismogram characteristics at $\Delta = 357$ km. The apparent velocities below this discontinuity increases to about 9 km/sec for P and 5 km/sec for S waves. Although these velocities are based on a single observation and are tentative until more seismic data become available from future impacts, the discontinuity is clearly a major structural boundary. It represents the lunar crust-mantle interface. If the high velocity in the outer portion of the lunar mantle persists it cannot be matched with terrestrial laboratory values.

Let us consider four petrologically feasible models of the lunar mantle to compare with the observed velocities. With some simplification, these models can be classified as: a)

olivine (SMITH et al., 1970), b) pyroxenite [orthopyroxene, clinopyroxene, olivine, spinel or garnet] (RINGWOOD and ESSENE, 1970; GREEN et al., 1970), c) peridotite (BIGGAR et al., 1971; O'HARA, et al., 1970), and d) a high pressure phase of anorthosite [grossularite, kyanite plus quartz] (ANDERSON and KOVACH, 1972). It is clear from laboratory values plotted in Figs. 9 and 10 and estimates made for lunar rocks by ANDERSON and KOVACH (1972) that the observed apparent velocities at the 70 km depth are greater than those of olivines, eclogites, pyroxenites (including garnet pyroxenites) and peridotites. Magnesium-rich olivines and eclogites with low FeO ratios are closest to the model. The high pressure form of anorthosite could have compressional velocities as high as 9.3 km/sec at 3 kb, but the mineralogical constraints for such a phase transformation are very stringent (BOETTCHER, 1971).

Before the upper mantle composition can be narrowed down on the basis of seismic results, it is necessary to have additional data to verify the observed apparent velocities. If the interface between the crust and mantle is dipping 3° eastward, the observed apparent P velocities may be 0.4 km/sec higher than the true velocity, thus reducing the upper mantle velocities to about 8.6 km/sec. The Apollo 16 S-IV-B is planned to impact to the west of the Apollo 12 and 14 stations and, if successful, it should resolve this uncertainty.

Any of the above petrological models implies a differentiated lunar mantle whose composition must vary with depth to satisfy mean density and moment of inertia constraints.

CONCLUSIONS

1. Seismic evidence directly shows that in the Fra Mauro Region of Oceanus Procellarum the moon has a layered crust and differentiated mantle.
2. The uppermost 25 km of the crust probably consists of basaltic material similar to that collected at Apollo 11, 12, 14 and 15 sites. A combination of very dry conditions and micro-cracks in rocks contribute to a rapid increase of velocity with depth, low attenuation, extensive scattering of seismic waves, and reverberating lunar seismograms.
3. At 25 km there is a change to what is believed to be a different composition. The most likely candidates on seismic and petrological grounds are gabbroic rocks such as anorthositic gabbro or gabbroic anorthosite.
4. At the investigated site, the lunar crust is about 65 km thick. The mantle below has very high apparent velocities based on a single impact recording. Any definitive interpretation of mantle mineralogy requires additional data.
5. All feasible mantle models compatible with petrological, chemical and seismic data as well as mass and moment of inertia constraints require a differentiated, radially inhomogeneous lunar mantle.

Note added in proofreading:

Seismic signals from the Apollo 16 S-IV-B impact were recently recorded at Apollo Lunar Stations 12, 14 and 15. The time and location of this impact were uncertain due to a loss of tracking capability. These parameters can be estimated, however, from the arrival times of P and S waves at the Apollo 12 and 14 stations. The first detectable motion at the Apollo 15 seismometer (at a distance of 1095 kilometers) indicates an average lunar mantle velocity of about 8 km/sec near a depth of 130 kilometers. Whether the high velocity (9 km/sec) zone in the uppermost portion of the mantle, reported above, is a universal feature or not cannot be determined from the new data.

The high frequencies (0.5-3.0 Hz) of compressional and shear waves observed at station 15 from the latest impact and also from deep moonquakes indicate the absence of high attenuation, precluding widespread melting in the outer several hundred kilometers of the lunar mantle.

ACKNOWLEDGEMENTS

We would like to thank Mr. E. Stolper for his assistance in the analysis of the data, Drs. G. Simmons and H. Wang, and Messrs. T. Todd and S. Baldrige for making their laboratory data available to us. Contributions of Drs. B. Julian, S. Solomon, and R. Wiggins are gratefully acknowledged.

This research was a cooperative effort of the Passive Seismic Experiment Team, led by Dr. G. Latham, in which the MIT group played the leading part. The work was supported by NASA Grants NGR22-009-123 and NAS9-12334.

REFERENCES

- ANDERSON, D.L. and KOVACH, R.L. (1972) The lunar interior. Earth Planet. Sci. Lett., in press.
- ANDERSON, O.L. and LIEBERMAN, R.C. (1966) Sound velocities in rocks and minerals. VESIAC State-of-the-Art Report, No. 7885-4-X, Willow Run Laboratories, University of Michigan, 189 pp.
- ANDERSON, O.L., SCHOLZ, C., SOGA, N., WARREN, N. and SCHREIBER, E. (1970) Elastic properties of a micro-breccia, igneous rock and lunar fines from Apollo 11 mission. Proc. Apollo 11 Lunar Sci. Conf., Geochim. Cosmochim. Acta Suppl. 1, Vol. 3, pp. 1959-1973. Pergamon.
- BIGGAR, G.M., O'HARA, M.J., PECKETT, A. and HUMPHRIES, D.J. (1971) Lunar lavas and the achondrites: petrogenesis of protohypersthene basalts in the maria lava lakes. Proc. Second Lunar Sci. Conf., Geochim. Cosmochim. Acta Suppl. 2, Vol. 1, pp. 617-643. MIT Press.
- BOETTCHER, A.L. (1971) The nature of the crust of the earth, with special emphasis on the role of plagioclase, in "The Structure and Properties of the Earth's Crust" (editor J.C. Heacock), Amer. Geophys. Un. Mono. 14, pp. 264-278.

- DAINTY, A. M. and ANDERSON, K. R. (1972) Seismic scattering in the moon and the earth. Abstract submitted to the 53rd Annual Meeting, American Geophysical Union.
- GAST, P.W. and MC CONNELL, JR., R.K., Evidence for initial chemical layering of the moon (abstract), "Revised Abstracts of the Third Lunar Science Conference", p. 289, January, 1972.
- GREEN, D. H., RINGWOOD, A.E., WARE, N.G., HIBBERSON, W.O., MAJOR, A., and KISS, E. (1971) Experimental petrology and petrogenesis of Apollo 12 basalts. Proc. Second Lunar Sci. Conf., Geochim. Cosmochim. Acta, Suppl. 2, Vol. 1, pp. 601-615. MIT Press.
- HELMBERGER, D.V. (1968) The crust-mantle transition in the Bering Sea. Bull. Seism. Soc. Amer. 58, 179-214.
- HELMBERGER, D.V. and WIGGINS, R.A. (1971) Upper mantle structure of midwestern United States. J. Geophys. Res. 76, 3229-3245.
- KANAMORI, H., NUR, A., CHUNG, D.H., WONES, D., and SIMMONS, G. (1970) Elastic wave velocities of lunar samples at high pressures and their geophysical implications. Science 167, 726-728.
- KANAMORI, H., MIZUTANI, H., and YAMANO, Y. (1971) Elastic wave velocity of Apollo 12 rocks at high pressures. Proc. Second Lunar Sci. Conf., Geochim Cosmochim. Acta Suppl. 2, Vol. 3, pp. 2323-2326. MIT Press.
- LATHAM, G., EWING, M., PRESS, F., SUTTON, G., DORMAN, J., NAKAMURA, Y., TOKSÖZ, N., DUENNEBIER, F., and LAMMLEIN, D.

- (1971) Passive seismic experiment. Apollo 14 Preliminary Science Report, NASA SP-272, pp. 133-161.
- LATHAM, G., EWING, M., PRESS, F., SUTTON, G., DORMAN, J., NAKAMURA, Y., TOKSÖZ, N., LAMMLEIN, D., and DUENNEBIER, F., Moonquakes and lunar tectonism -- results from the Apollo Passive Seismic Experiment (abstract), "Revised Abstracts of the Third Lunar Science Conference", p. 478, January, 1972.
- LSPET (Lunar Sample Preliminary Examination Team) The Apollo 15 lunar samples: a preliminary description. Science 175, 363-375.
- MIZUTANI, H., FUJII, N., HAMANO, Y., OSAKO, M. and KANAMORI, H. Elastic wave velocities and thermal diffusivities of Apollo 14 rocks (abstract), "Revised Abstracts of the Third Lunar Science Conference", p. 547, January, 1972.
- NAKAMURA, Y., LATHAM, G. V., EWING, M., and DORMAN, J. (1970) Lunar seismic energy transmission. EOS 51, 776.
- NUR, A. and SIMMONS, G. (1969) The effect of saturation on velocity in low porosity rocks. Earth Planet. Sci. Lett. 7, 183-193.
- O'HARA, M.J., BIGGAR, G.M., RICHARDSON, S.W., JAMIESON, B.G., and FORD, C.E. (1970) The nature of seas, mascons, and the lunar interior in the light of experimental studies. Proc. Apollo 11 Lunar Sci. Conf., Geochim. Cosmochim Acta Suppl. 1, Vol. 1, pp. 695-710. Pergamon.
- PRESS, F., (1966) Seismic velocities. Handbook of Physical Con-

stants, S. P. Clark, Editor, Geol. Soc. Amer. Mem. 97,
p. 195.

REID, A.M., RIDLEY, W.I., WARNER, J., HARMON, R.S., BRETT, R.,
JAKES, P., and BROWN, R.W., Chemistry of Highland and Mare
basalts as inferred from glasses in the lunar soils (ab-
stract), "Revised Abstracts of the Third Lunar Science
Conference", p. 640, January, 1972.

RINGWOOD, A.E., and ESSENE, E.J. (1970) Petrogenesis of Apollo
11 basalts, internal constitution and origin of the moon.
Proc. Apollo 11 Lunar Sci. Conf., Geochim. Cosmochim. Acta
Suppl. 1, Vol. 1, pp. 769-799. Pergamon.

SJORGEN, W.L., GOTTLIEB, P., MULLER, P.M., and WOLLENHAUPT, W.
(1972) Lunar gravity data via Apollo 14 Doppler radio
tracking. Science 175, 165-168.

SMITH, J.V., ANDERSON, A. T., NEWTON, R.C., OLSEN, E.J., WYLLIE,
P.J., CREWE, A.V., ISAACSON, M.S., and JOHNSON, D. (1970)
Petrologic history of the moon inferred from petrography,
mineralogy, and petrogenesis of Apollo 11 rocks. Proc.
Apollo 11 Lunar Sci. Conf., Geochim. Cosmochim. Acta Suppl.
1, Vol. 1, pp. 897-925. Pergamon.

TITTMANN, B.R., ABDEL-GAWAD, M., and HOUSLEY, R.M., Rayleigh
wave studies of lunar and synthetic rocks (abstract),
"Revised Abstracts of the Third Lunar Science Conference",
p. 755, January, 1972.

TODD, T., WANG, H., BALDRIDGE, W.S., and SIMMONS, G. (1972)

Elastic properties of Apollo 14 and 15 rocks, this volume.

TOKSÓZ, M.N., PRESS, F., ANDERSON, K., DAINTY, A., LATHAM, G., EWING, M., DORMAN, J., LAMMLEIN, D., NAKAMURA, Y., SUTTON, G., and DUENNEBIER, F. (1972a) Velocity structure and properties of the lunar crust. The Moon, in press.

TOKSÓZ, M.N., PRESS, F., ANDERSON, K., DAINTY, A., LATHAM, G., EWING, M., DORMAN, J., LAMMLEIN, D., SUTTON, G., DUENNEBIER, F., and NAKAMURA, Y. (1972b) Lunar crust: structure and composition. Submitted to Science.

WALKER, D., LONGHI, J., and HAYS, J.F., Experimental petrology and origin of Fra Mauro rocks and soil (abstract), "Revised Abstracts of the Third Lunar Science Conference", p. 770, January, 1972.

WANG, H., TODD, T., WEIDNER, D., and SIMMONS, G. (1971) Elastic properties of Apollo 12 rocks. Proc. Second Lunar Sci. Conf., Geochim. Cosmochim. Acta Suppl. 2, Vol. 3, pp. 2327-2336. MIT Press.

WARREN, H., SCHREIBER, E., SCHOLZ, C., MORRISON, J.A., NORTON, P. R., KUMAZALA, M., and ANDERSON, O.L. (1971) Elastic and thermal properties of Apollo 12 and Apollo 11 rocks. Proc. Second Lunar Sci. Conf., Geochim. Cosmochim. Acta Suppl. 2, Vol. 3, pp. 2345-2360. MIT Press.

WOOD, J.A. (1970) Petrology of the lunar soil and geophysical implications. J. Geophys. Res. 75, 6497-6513.

WOOD, J.A., MARVIN, U.B., REID, JR., J.B., TAYLOR, G.J., BOWER,
J.F., POWELL, B.N., and DICKEY, JR., J.S. (1971) Mineralogy
and petrology of the Apollo 12 lunar sample. Smithsonian
Astrophysical Obs. Spec. Rep. 333, 272 pp.

FIGURE CAPTIONS

- Fig. 1 Location map showing the region (in frame) of the moon where most of the seismic observations have been made. Three operating seismic stations are shown as black triangles. Enlarged picture on the right shows Apollo 12 and Apollo 14 seismic stations, impact points and seismic wave paths.
- Fig. 2 A composite illustration of vertical components of seismograms recorded from all artificial impacts. Notation "LM 14 at 14" means LM-14 impact recorded at Apollo 14 seismic station. "dmax" is the amplitude normalization scale; to obtain true relative amplitudes, seismogram amplitudes must be multiplied by this factor. Distance is in degrees; 1 degree = 30.3 km. Arrows indicate the first arrival. Note the change of character of S-IV-B seismograms with distance.
- Fig. 3 Seismograms of the Apollo 13 S-IV-B impact recorded at the Apollo 12 station and the LM-14 impact recorded at the Apollo 12 station. R, T, and Z indicate radial, transverse, and vertical components of the motion, respectively. Each seismogram is band-pass

filtered at two period intervals: 1-4 sec and 3-15 sec. P, PP, PPP, S and SS arrivals are shown.

Fig. 4 Travel-times, amplitudes, and ray paths for P wave pulses. "Second arrival" P denotes a relatively large amplitude pulse that arrives after P which is associated with a travel-time cusp. PP and PPP are surface reflected phases. Lines are theoretical curves for velocity model given in Fig. 7. "D.U." signifies digitization unit. Seismic ray paths inside the moon (at the bottom) show the effects of high velocity gradients. Ray crossings correspond to multiplication of travel-times. High density of rays indicates focusing of energy and hence large amplitudes.

Fig. 5 Travel-times and amplitudes of S waves. Theoretical curves are for the velocity model shown in Fig. 7. All other designations same as those in Fig. 4.

Fig. 6 Observed (solid line) and synthetic (dashed line) P wave seismograms for three S-IV-B impacts recorded at station 12. The change in seismic pulse shapes

and relative amplitudes of first and later arrivals with increasing distance is obvious. At 357 km the first two peaks of observed seismograms are noise pulses and can be clearly identified as such in unfiltered seismograms.

Fig. 7 Compressional (solid line) and shear (dashed line) velocity versus depth profiles for the moon in the vicinity of Fra Mauro.

Fig. 8 Compressional and shear velocity versus pressure curves (laboratory data) for dry and water-saturated Casco granite (porosity = 0.7%). (after NUR and SIMMONS, 1971).

Fig. 9 Observed compressional velocity profile (hatched lines) and velocities of lunar and terrestrial rocks measured in the laboratory as a function of pressure. On the left, lunar rocks are identified by a sample number. "Terrestrial basalts" is an average value for basalts of the earth. On the right, all laboratory data are terrestrial. Two curves for each rock type mark the typical lower and upper boundaries of velocities for such rock types.

Fig. 10 (Left) Observed shear velocity profile (hatched line) and velocities of lunar and terrestrial rocks measured in the laboratory. (Right) Poisson's ratio versus depth curve for the moon (computed from P and S velocity profiles) and those of lunar rocks and terrestrial dry and saturated granite.

TABLE I

A. Coordinates of Seismic Stations and Impact Points and Relevant Distances.

Stations and Impacts	Coordinates (degrees)	Distances (in km) from		
		Apollo 12 Site	Apollo 14 Site	Apollo 15 Site
Apollo 12 Site	3.04S,23.42W	-	-	-
Apollo 14 Site	3.65S,17.48W	181	-	-
Apollo 15 Site	26.08N,3.66E	1188	1095	-
Apollo 12 LM Impact	3.94S,21.20W	73	-	-
Apollo 13 S-IV B Impact	2.75S,27.86W	135	-	-
Apollo 14 S-IV B Impact	8.00S,26.06W	170	-	-
Apollo 14 LM Impact	3.42S,19.67W	114	67	-
Apollo 15 S-IV B Impact	1.36S,11.77W	357	186	-
Apollo 15 LM Impact	26.36N,0.25E	1130	1049	93

TABLE I

B. Impact Parameters

Impact	Date day-month-yr	Time (hr:min:sec)	Velocity (km/sec)	Mass (kg)	Kinetic Energy (ergs)	Angle from Horizontal (degrees)
Apollo 12 LM	20-11-69	22:17:17.7	1.68	2383	3.36×10^{16}	3.7
Apollo 14 LM	7-02-71	00:45:25.7	1.68	2303	3.25×10^{16}	3.6
Apollo 15 LM	3-08-71	03:03:37.0	1.70	2385	3.44×10^{16}	3.2
Apollo 13 S-IV B	15-04-70	01:09:41.0	2.58	13925	4.63×10^{17}	76
Apollo 14 S-IV B	4-02-71	07:40:55.4	2.54	14016	5.54×10^{17}	69
Apollo 15 S-IV B	29-07-71	20:58:42.9	2.58	13852	4.61×10^{17}	62

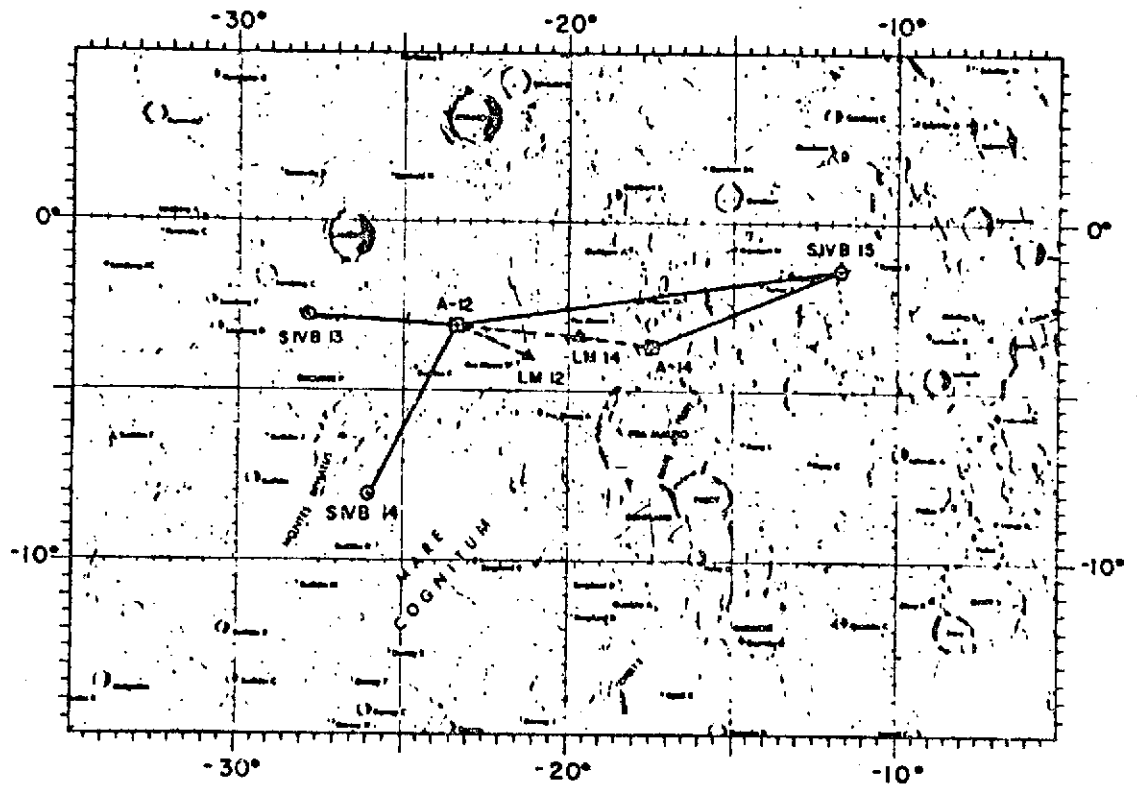
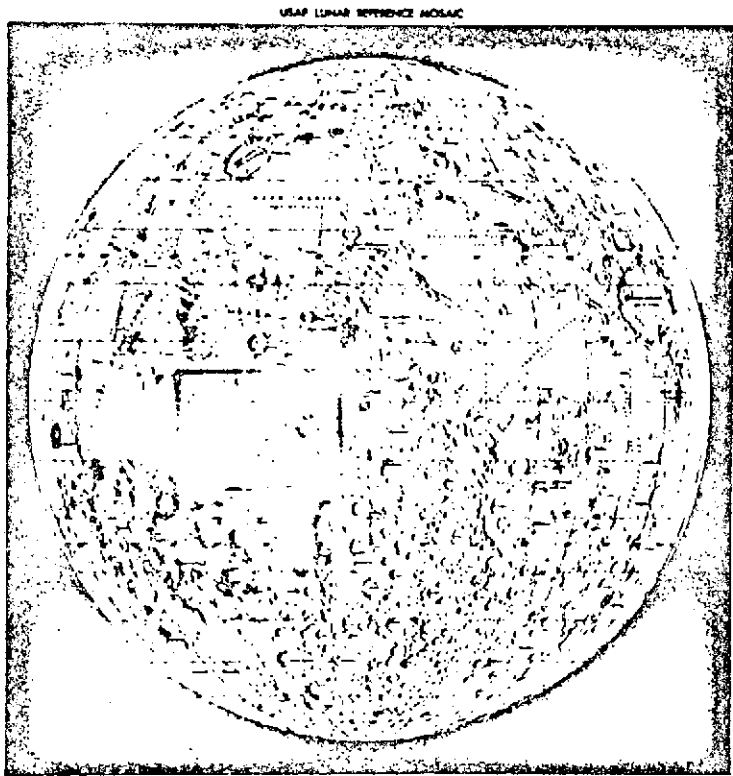


Fig. 1

TIME AFTER IMPACT (MINUTES)

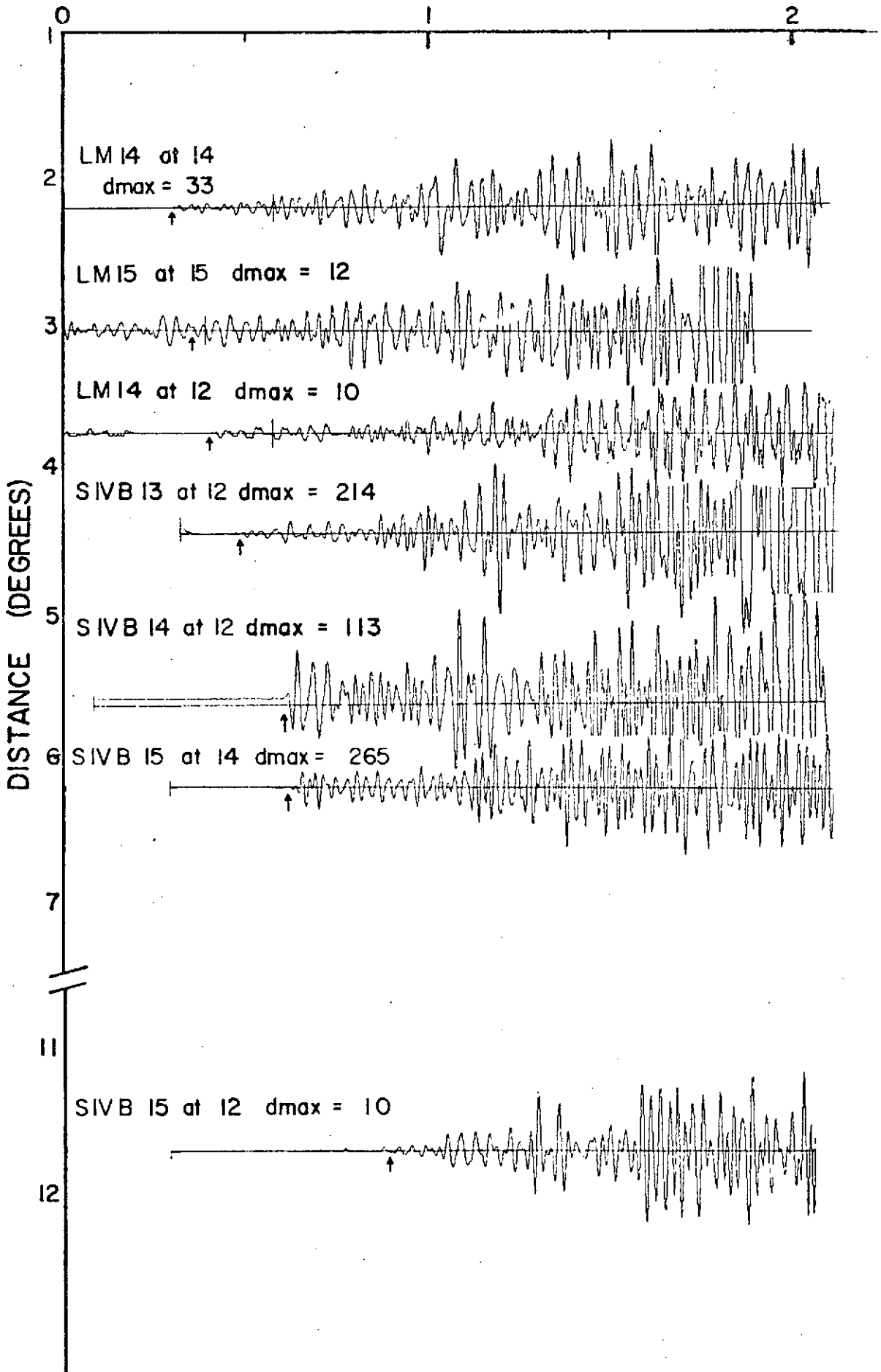
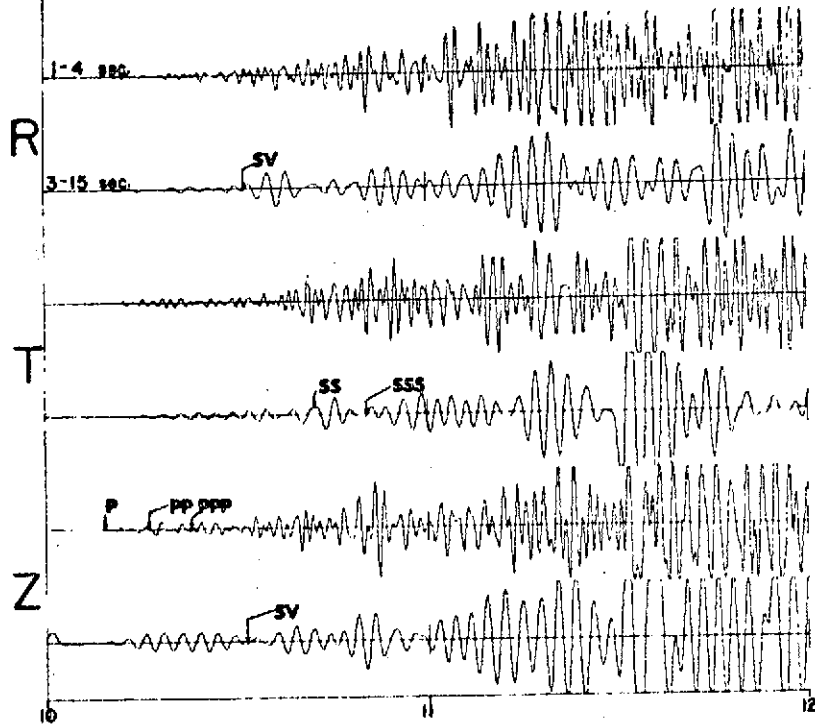


Fig. 2

APRIL 15, 1970

SIVB-13 Impact ALSEP 12 01:10.0 GMT



FEBRUARY 7, 1971

LM 14 Impact ALSEP 12 00:45.7 GMT

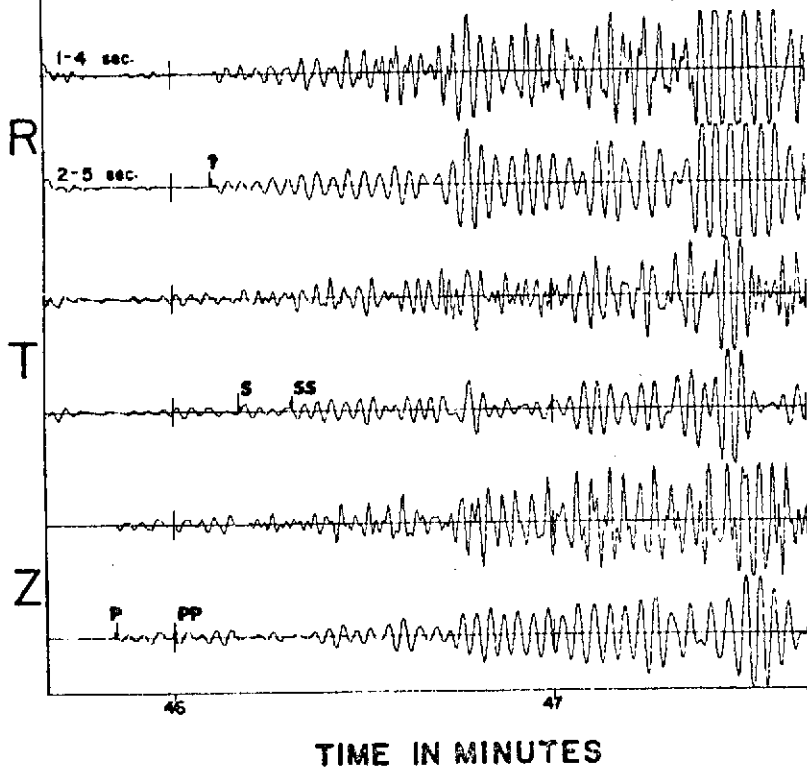


Fig. 3

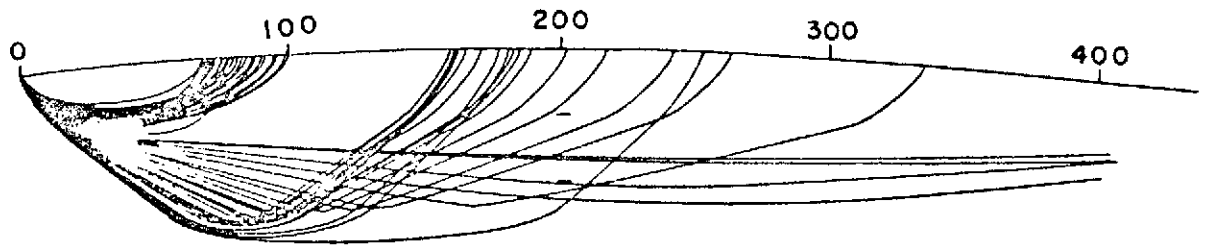
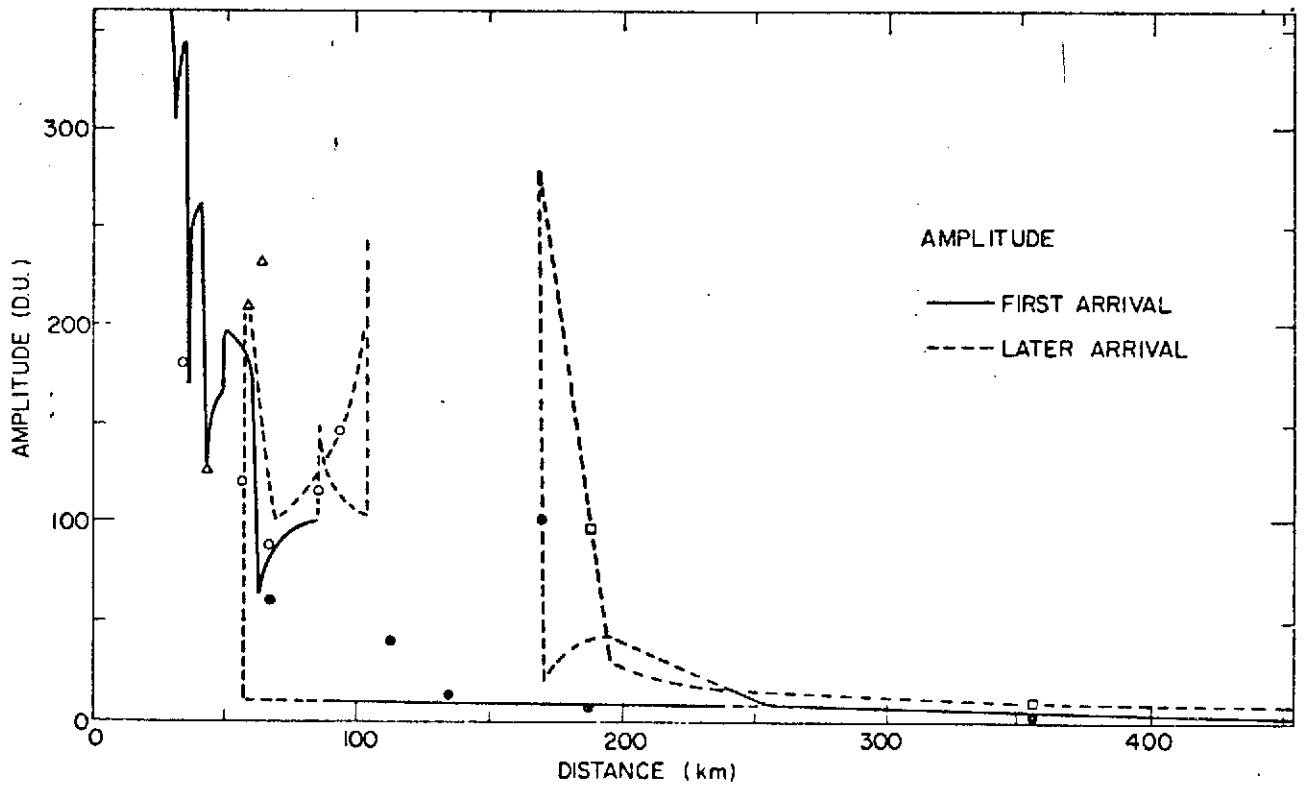
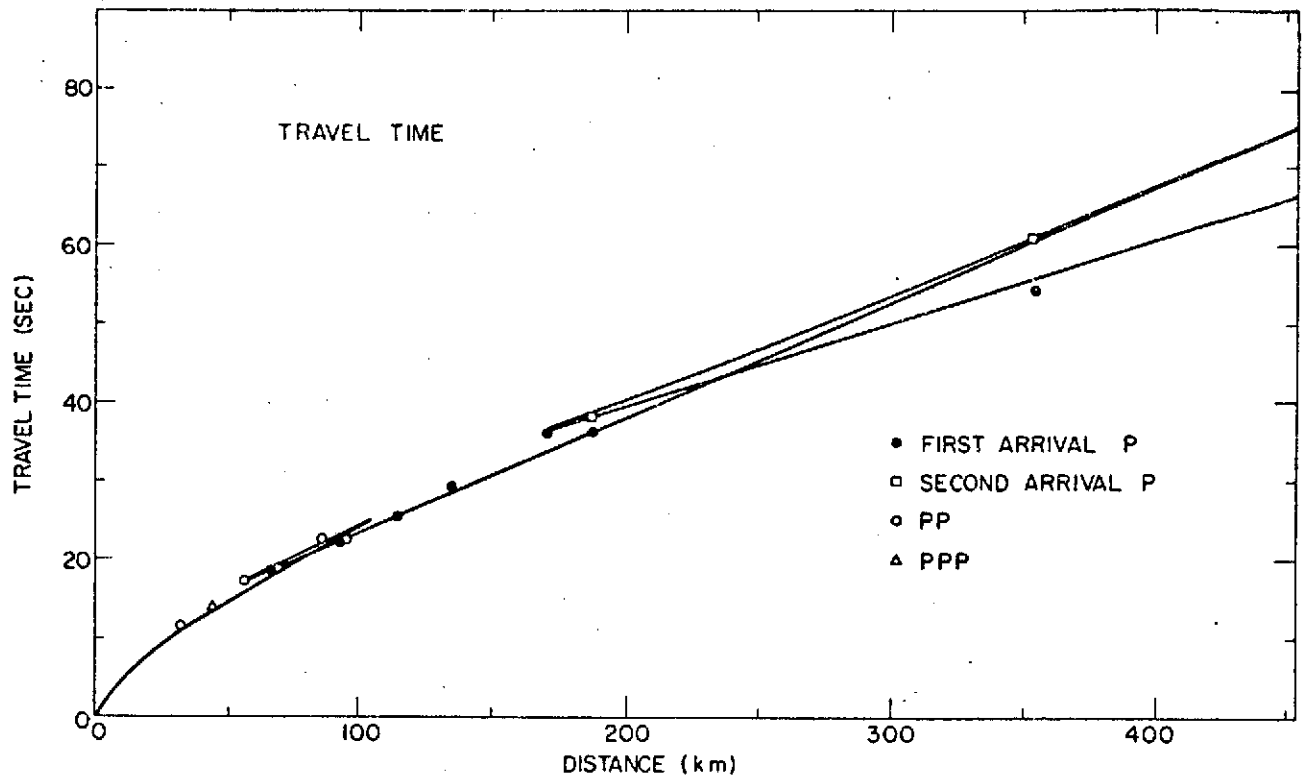


Fig. 4

DEPTH 100 - km

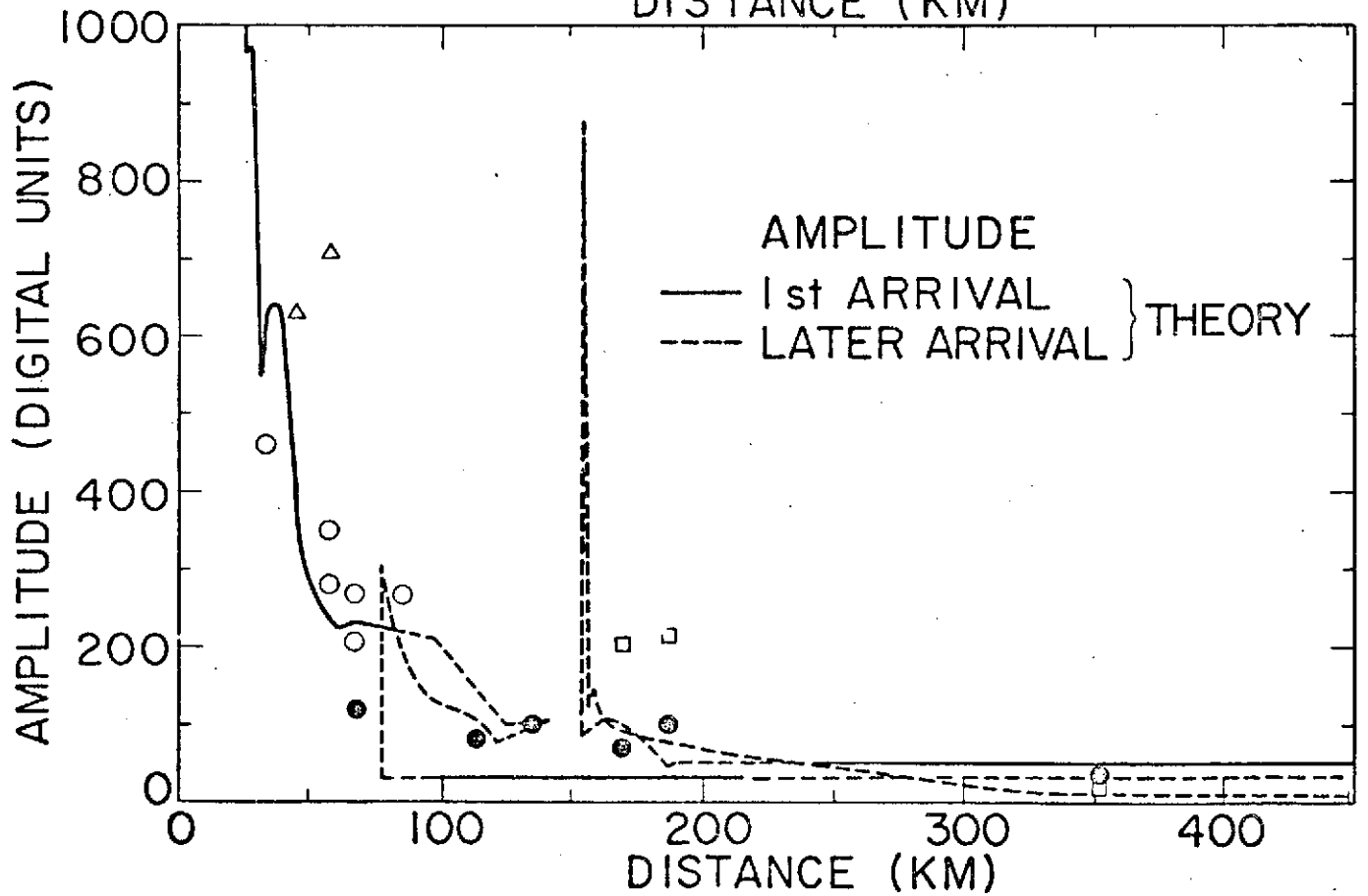
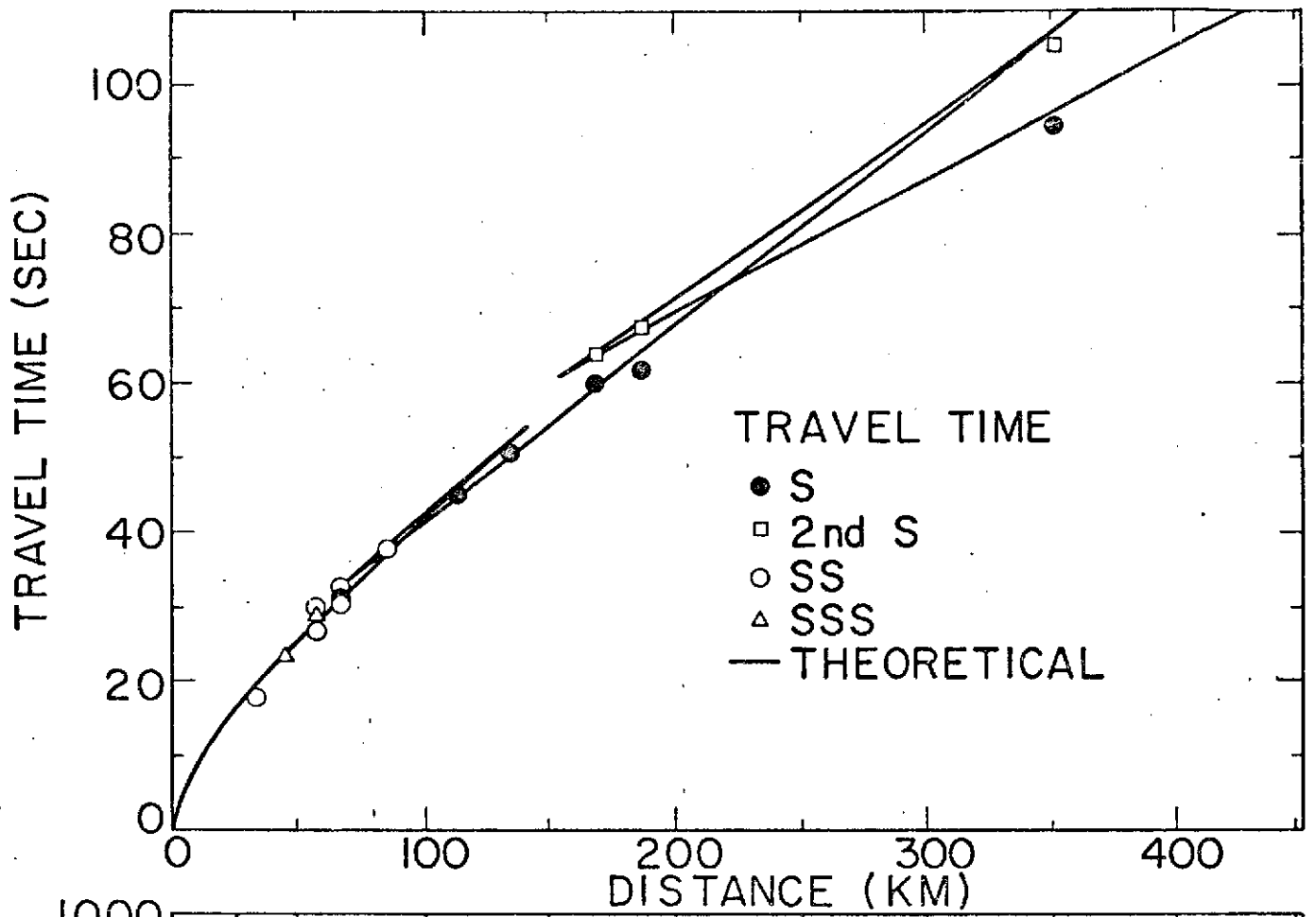


Fig. 5

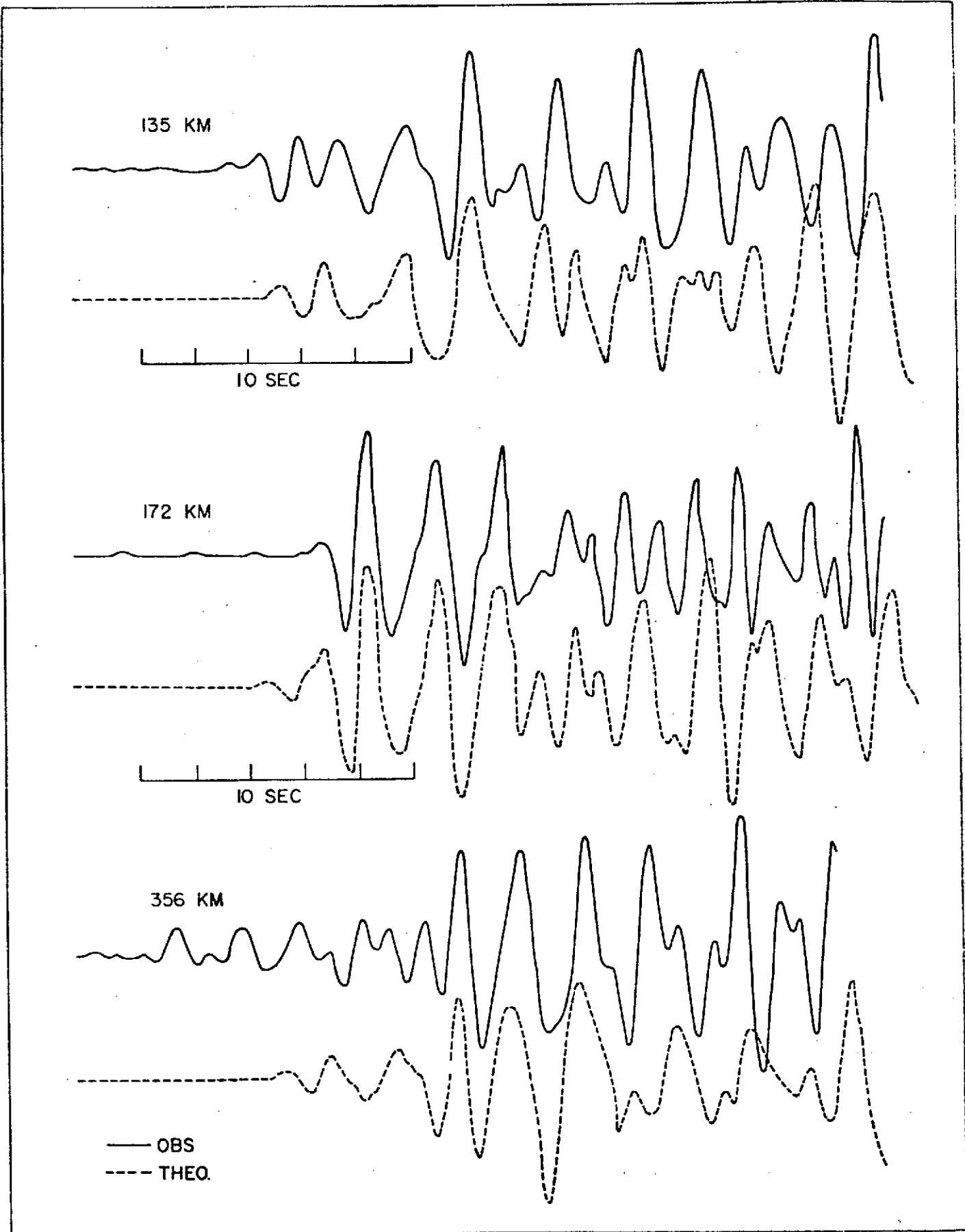


Fig. 6

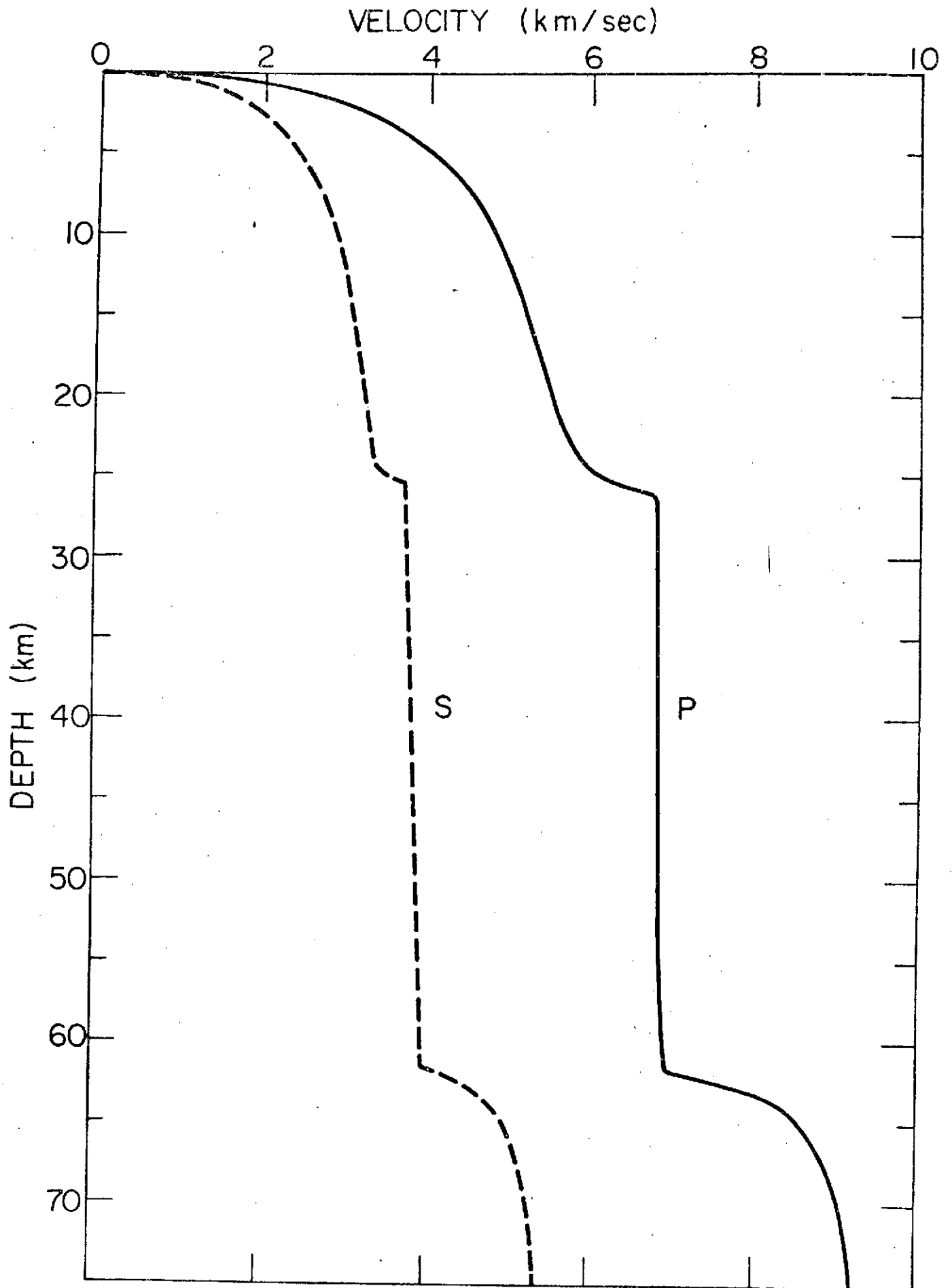


Fig. 7

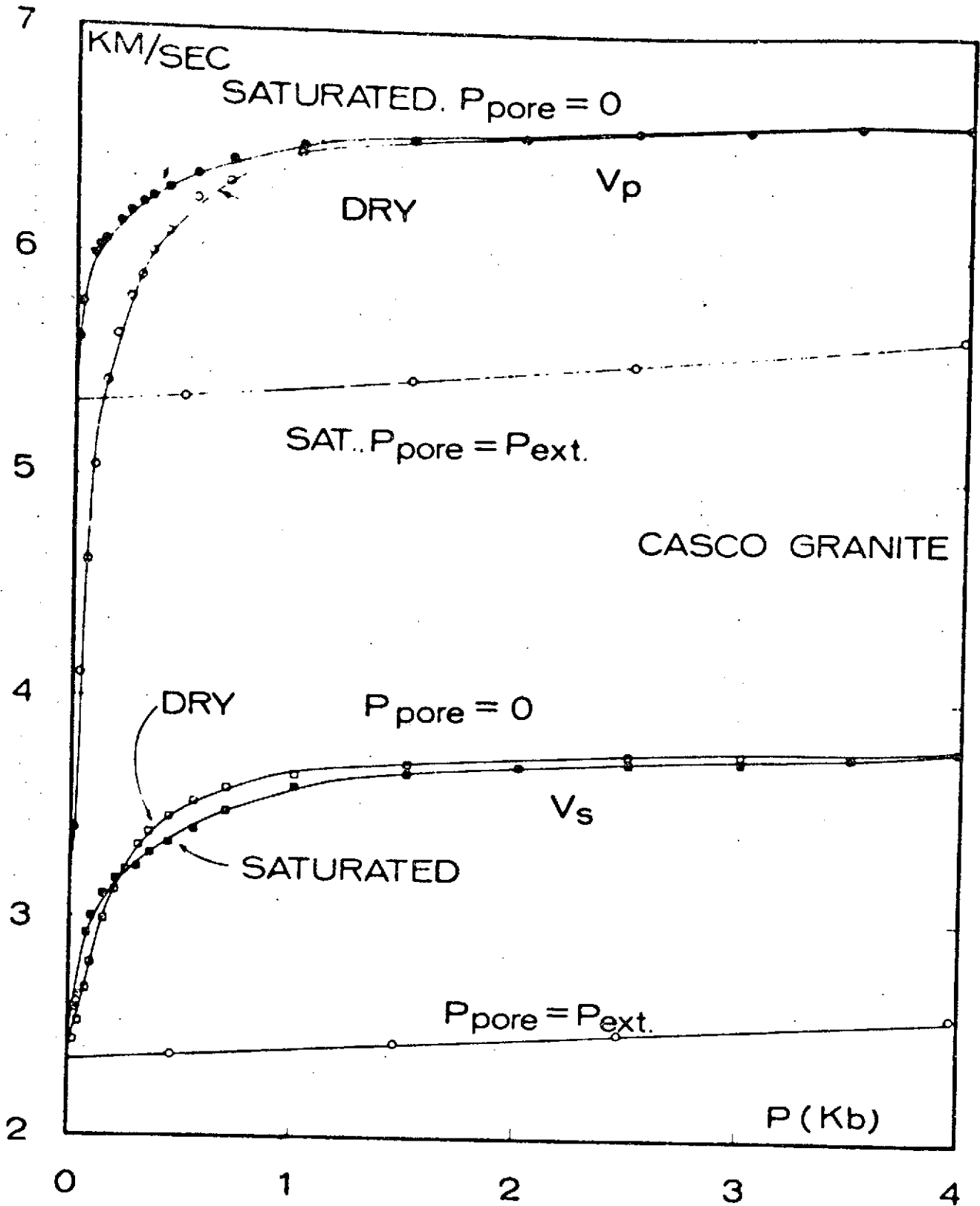


Fig. 8

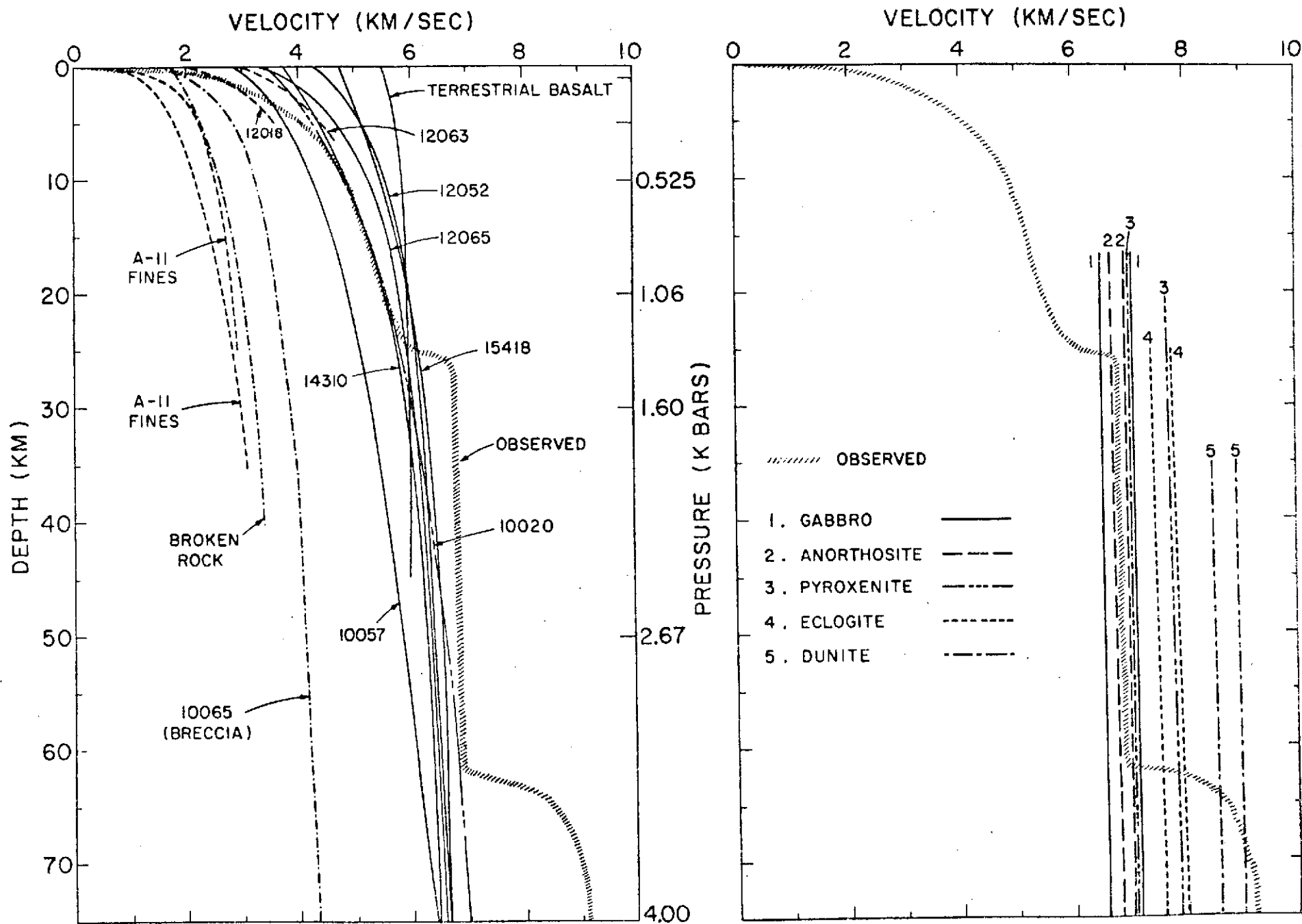


Fig. 9

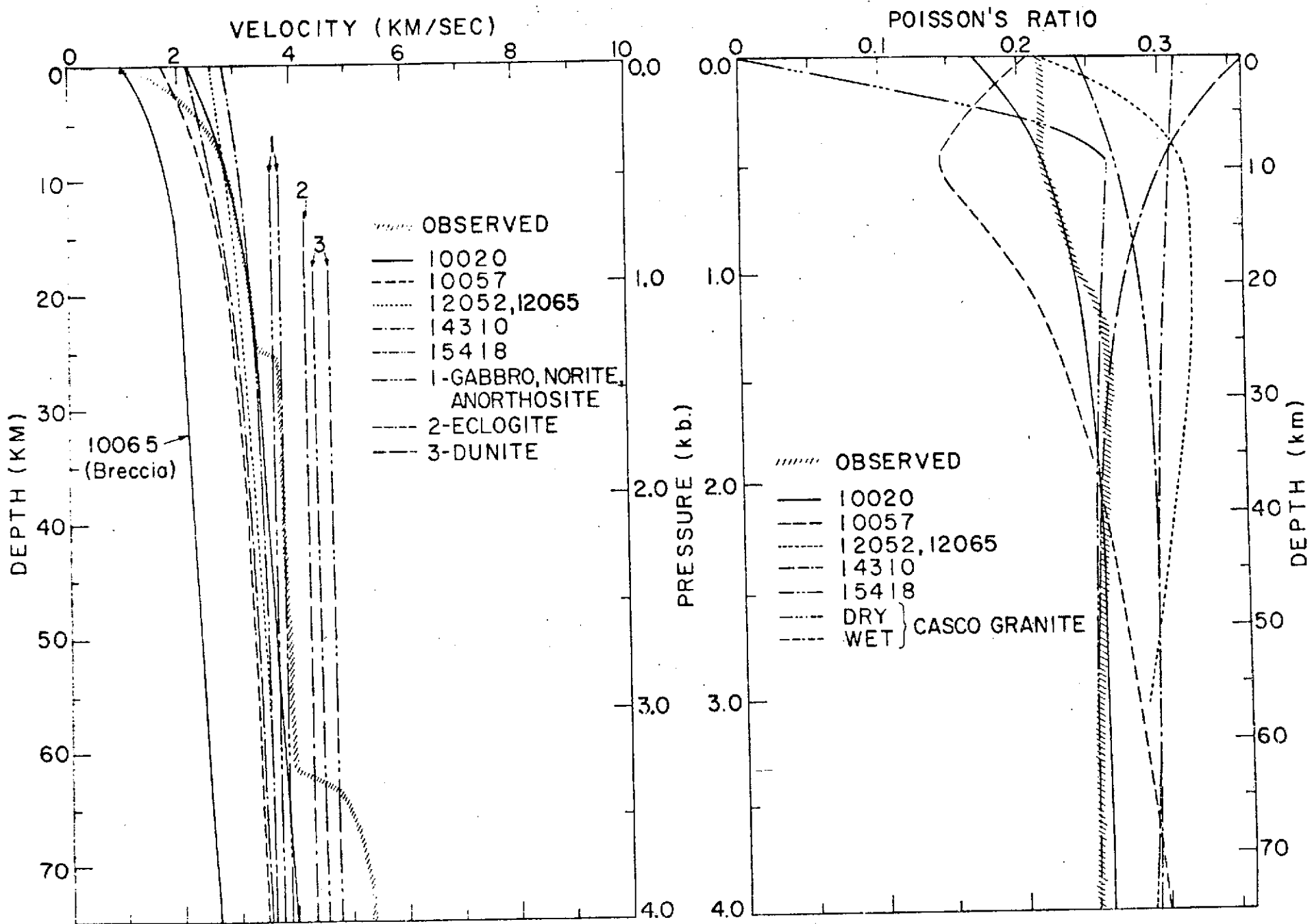


Fig. 10

Chapter 3

SEISMIC SCATTERING IN THE MOON AND THE EARTH

by

Anton M. Dainty and Kenneth R. Anderson
Department of Earth and Planetary Sciences
Massachusetts Institute of Technology

One of the first discoveries of the Apollo Passive Seismic Experiment was the unexpectedly long and reverberating seismic train observed for artificial and natural impacts and moonquakes.

Figure 1 is a seismogram, albeit plotted in a somewhat unusual form. It represents the energy envelope, heavily smoothed, for seismic energy in the band 0.42 - 0.48 Hz received at the Alsep 12 Station from the impact of the Apollo 15 Saturn IV-B booster 360 km away. A logarithmic scale of energy is used, referenced to some arbitrary energy; note the time scale--an hour of data is presented and after an hour the energy is down by a factor of 10 from the peak.

To explain this phenomenon, Latham et al proposed the model shown in Figure 2. There is a surface layer where seismic energy is intensely scattered; this process may be considered as diffusion of the energy, analogous to the diffusion of molecules in the kinetic theory of gases. Below this, seismic energy propagates in a more conventional manner. Energy may travel from a surface impact to a surface receiver either by direct diffusion through the layer, or by diffusion down through the layer, propagation through the underlying medium, and diffusion back up through the layer, as shown in Figure 2. Latham et al proposed this model on the basis of source-receiver separations comparable to the layer thickness--we wish to examine the case of large source-receiver

separations. In this case, for an impulsive surface source, such as impact, energy diffusing directly through the layer may be ignored, and only energy propagated through the underlying medium considered. Assuming that the propagation time through the underlying medium is negligible compared to the time of diffusion through the scattering layer, the energy envelope $e(t)$ at the receiver is the convolution of a function $f(t)$ representing near-source diffusion and a similar near-receiver diffusion function $g(t)$. If we assume that $f(t) = g(t)$, we may calculate $f(t)$ from the observed energy envelope of an impact by Fourier transforming $e(t)$, taking the square root and retransforming back into the time domain. In addition, it is possible to measure $g(t)$ directly by examining the energy envelopes of moonquakes. These moonquakes are believed to have focal depths greater than the bottom of the scattering layer--thus, the energy envelope $e(t) = g(t)$, since the signal is diffused only near the receiver.

Having obtained the near-source diffusion function $f(t)$, we would like to interpret it. To do this, the following rather simple theoretical model has been used. The source is considered as an impulse at the surface, and energy is considered to diffuse out three-dimensionally until it reaches a radius r equal to the scattering-layer thickness, after which it propagates. $f(t)$ is then given by the Green's function for this diffusion problem (with dissipation) which is shown in Figure 3--this function is

given in Latham et al. The parameters of the problem are: firstly, the diffusivity z , which, using the concepts of the kinetic theory of gases, is the product of twice the seismic velocity V in the layer and the mean free path of seismic energy ℓ , and secondly, the Q of the scattering-layer material.

Figure 4 shows some data. The solid line is the near-source diffusion function determined as described for the impact shown in Figure 1 (this is the furthest artificial impact available). Also shown as a dashed line is the energy envelope of a moonquake and as a dotted line a theoretical curve. Note once again the band 0.42 - 0.48 Hz. We think you will agree that all three curves look reasonably similar, supporting the picture presented earlier of how a long, reverberating train of seismic energy occurred. For the theoretical calculation, the two numbers that are obtained are the value of the square of the scattering-layer thickness over the diffusivity, r^2/z and the Q . r^2/z is rather hard to interpret at this time, but the high value of Q , 3600, confirms previous estimates of this quantity.

Figure 5 is similar to Figure 4 but for a frequency band around 1 Hz. Note that r^2/z has decreased--the scattering layer may get effectively thinner for higher frequencies. Note also that the theoretical curve falls below both observed curves at large times. Since this portion of the theoretical curve is controlled by the Q , it appears that a higher Q is

required. This apparent frequency dependence of Q may be due to the fact that the loss of energy in the scattering layer represented by Q may be partly due to energy being scattered out of the scattering layer and lost, not simply intrinsic losses in the medium.

A conclusion drawn widely after the discovery of reverberating seismograms on the moon was "look how different the seismic transmission properties of the moon are from those of the earth." We wish to advance the proposition that they are not as different as you might think. In particular, we think the big difference is the high Q of the moon, due perhaps to the lack of volatiles, rather than the presence or absence of scatterers. The top part of Figure 6 shows a recording of the nuclear explosion Half Beak at 310 km distance, with a frequency around 1 Hz-- rather similar distance and frequency to the impact discussed earlier; the envelope of the seismogram has also been drawn. Note the time scale. The bottom half shows the result of multiplying by $e^{\omega t/2Q}$ in an attempt to correct the seismogram to the case of infinite Q (no dissipation). The value of Q used was 107; this value was chosen because it appeared to correct the P coda to a constant value. We then see that firstly, intense scattering is in fact taking place and secondly, the seismogram shows a tendency to "build up" like the moon seismograms in their early portion. Note, for example, that the P wave, the largest burst of

energy on the original seismogram, is the smallest on the modified seismogram.

This suggests that perhaps only the presence of water, lowering Q , on the earth has permitted the development of crustal seismology--otherwise, crustal seismograms would be as reverberating as those on the moon.

Reference

Latham, G., M. Ewing, F. Press, G. Sutton, J. Dorman,
Y. Nakamura, N. Toksöz, F. Duenebier, and D. Lammlein,
"Passive Seismic Experiment", Apollo 14 Preliminary
Science Report, NASA SP-272, 133-161, 1971.

Acknowledgements

The authors would like to thank Professor M. N. Toksöz for his advice and encouragement, also other members of the Passive Seismic Experiment team--names are given in the reference. This research was supported by NASA under Contracts NAS 9-12334; NGR 22-009-123 at MIT.

Figure Captions

- Figure 1. Energy envelope (smoothed) of the S-IV-B 15 booster impact recorded at the Apollo 12 station in the frequency band 0.42 - 0.48 Hz. Time zero is impact time, and the range is 357 km.
- Figure 2. Seismic model for energy envelope at large range, assuming source is impulse.
- Figure 3. Near source region, impulsive source, for calculation of source scattering function $f(t)$.
- Figure 4. Observed source scattering function $f(t)$ derived from envelope shown in Figure 1 (solid line), observed moonquake envelope (dashed line), and theoretical curve (dotted line), for frequency band 0.42 - 0.48 Hz. The parameters for the theoretical curve are $r^2/z = 585$ sec., $Q = 3600$, where r , z , and Q are defined in Figure 3.
- Figure 5. Same as Figure 4, for frequency band 0.93 - 1.07 Hz. The parameters for the theoretical curve are $r^2/z = 410$ sec, $Q = 3600$.
- Figure 6. Top, seismogram from nuclear explosion Half-Beak at a range of 310 km. Bottom, seismogram corrected for attenuation ($Q = 107$).

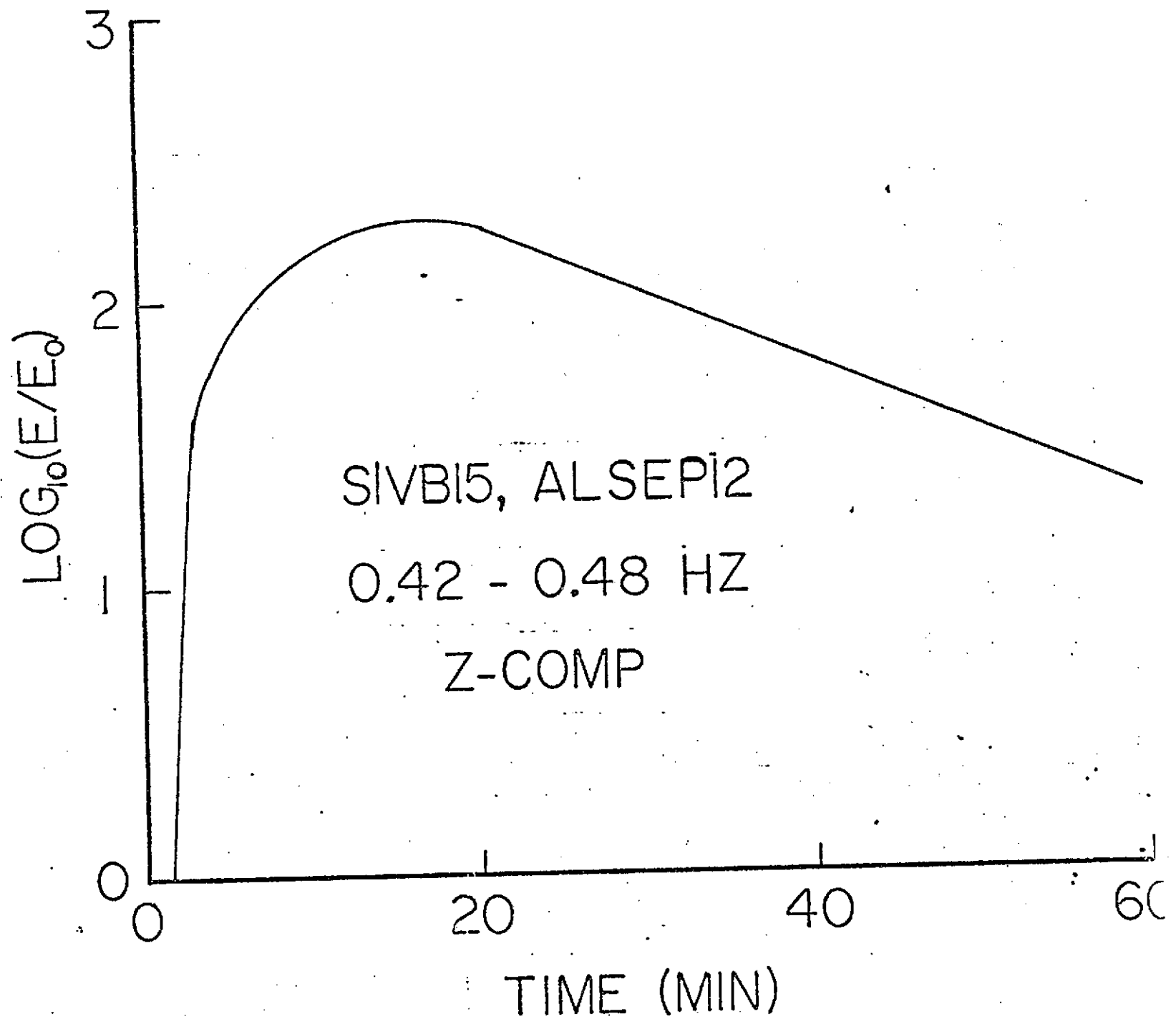
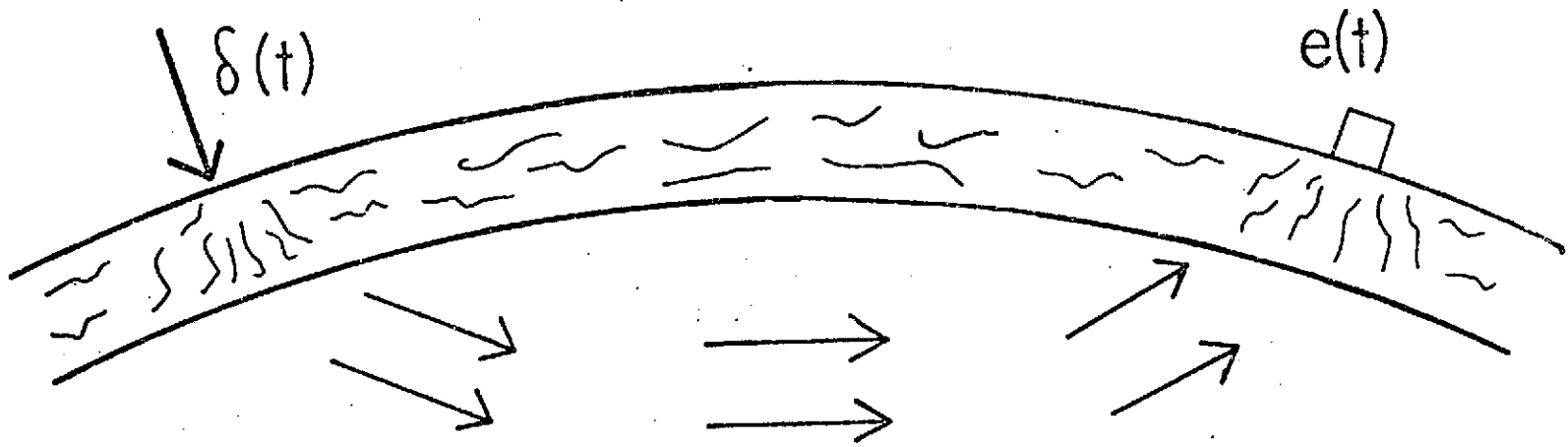


Figure 1.



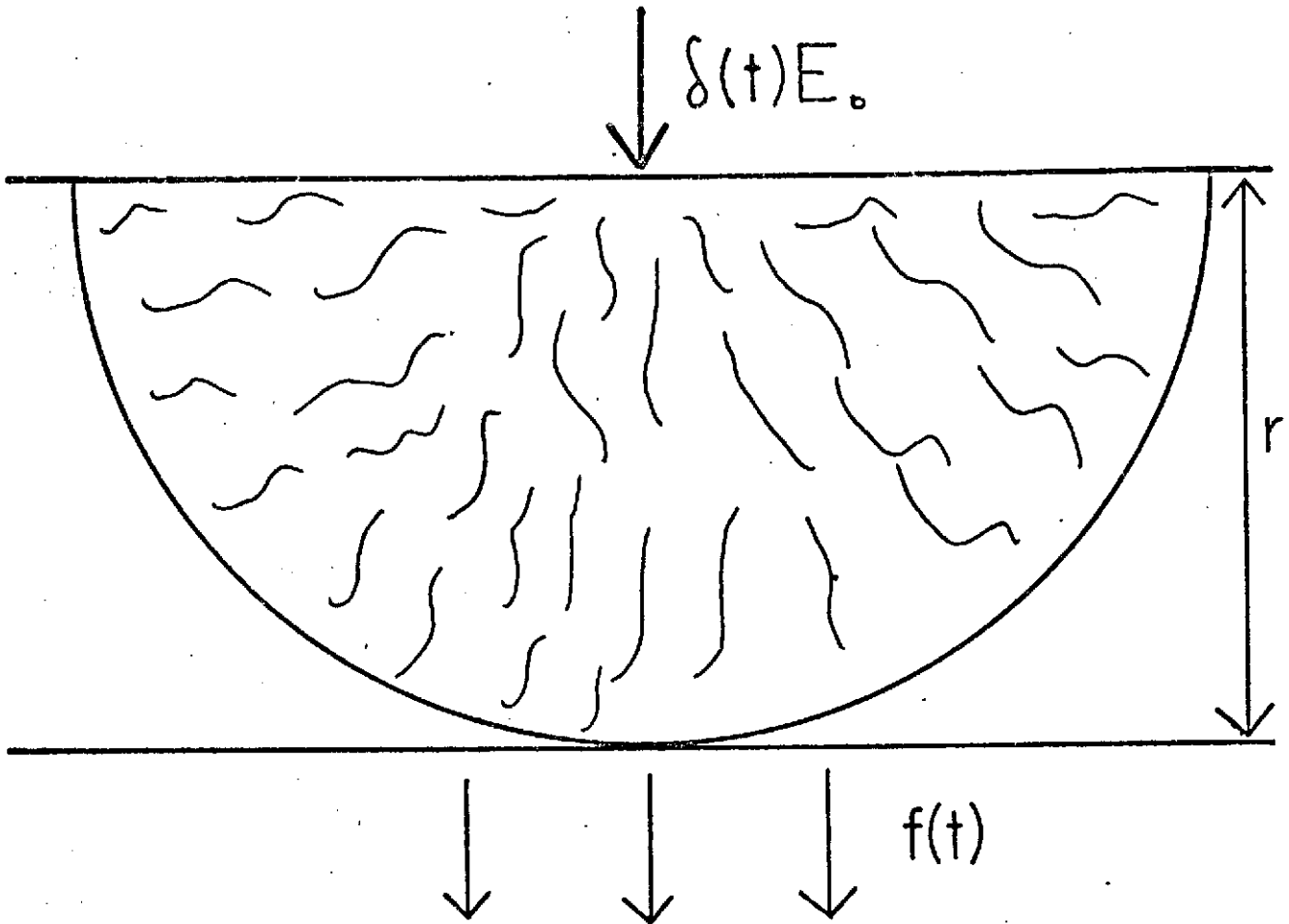
LARGE SEPARATION:

$$e(t) = f(t) * g(t)$$

RECIPROCITY:

$$f(t) = g(t)$$

Figure 2.



$$f(t) = \frac{2E_0}{(\pi z t)^{3/2}} \exp\left[\frac{-r^2}{z t} - \frac{w t}{Q}\right]$$

$z = 2vl =$ DIFFUSIVITY

$v =$ SEISMIC VELOCITY

$l =$ MEAN FREE PATH

Figure 3.

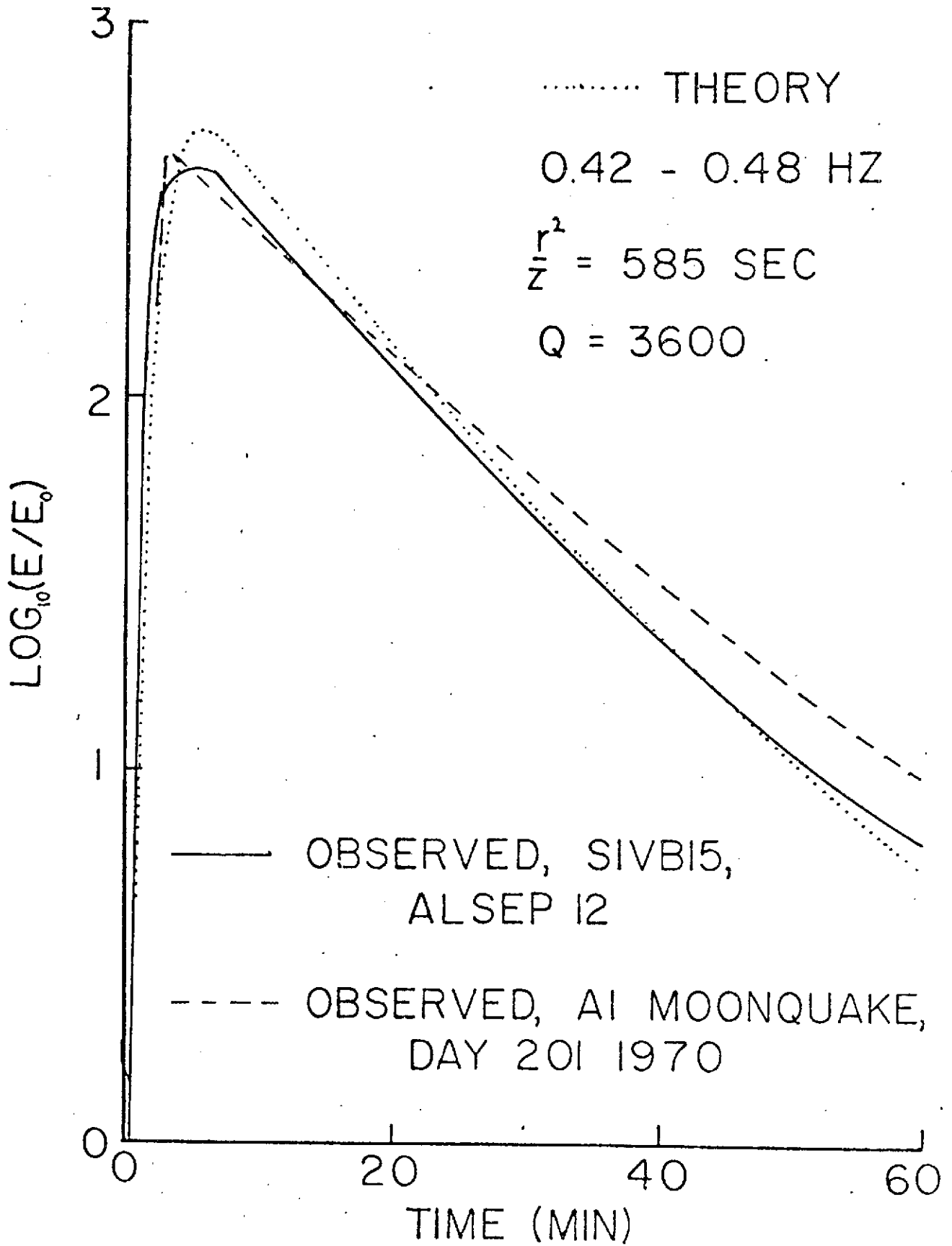


Figure 4.

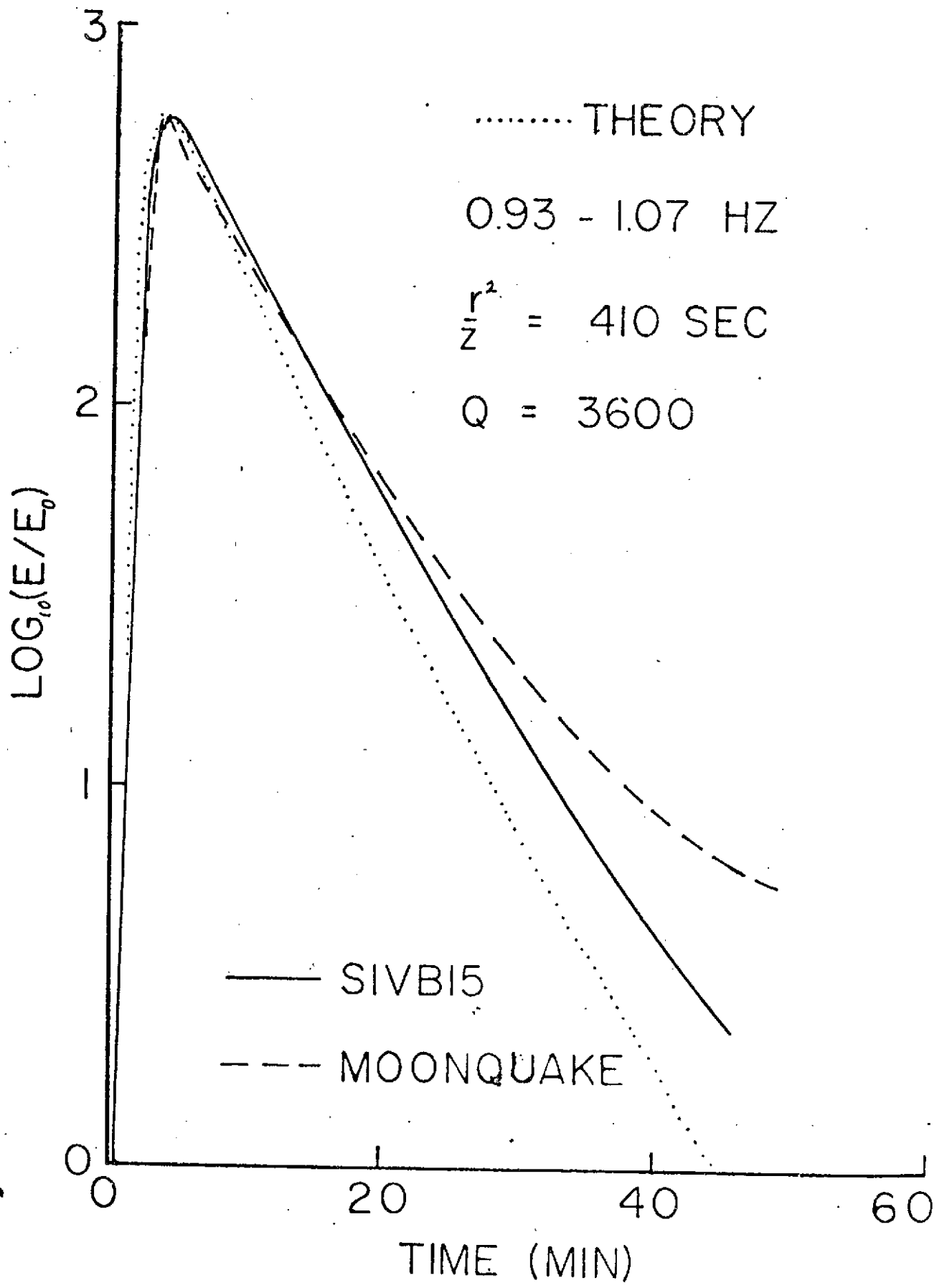


Figure 5.

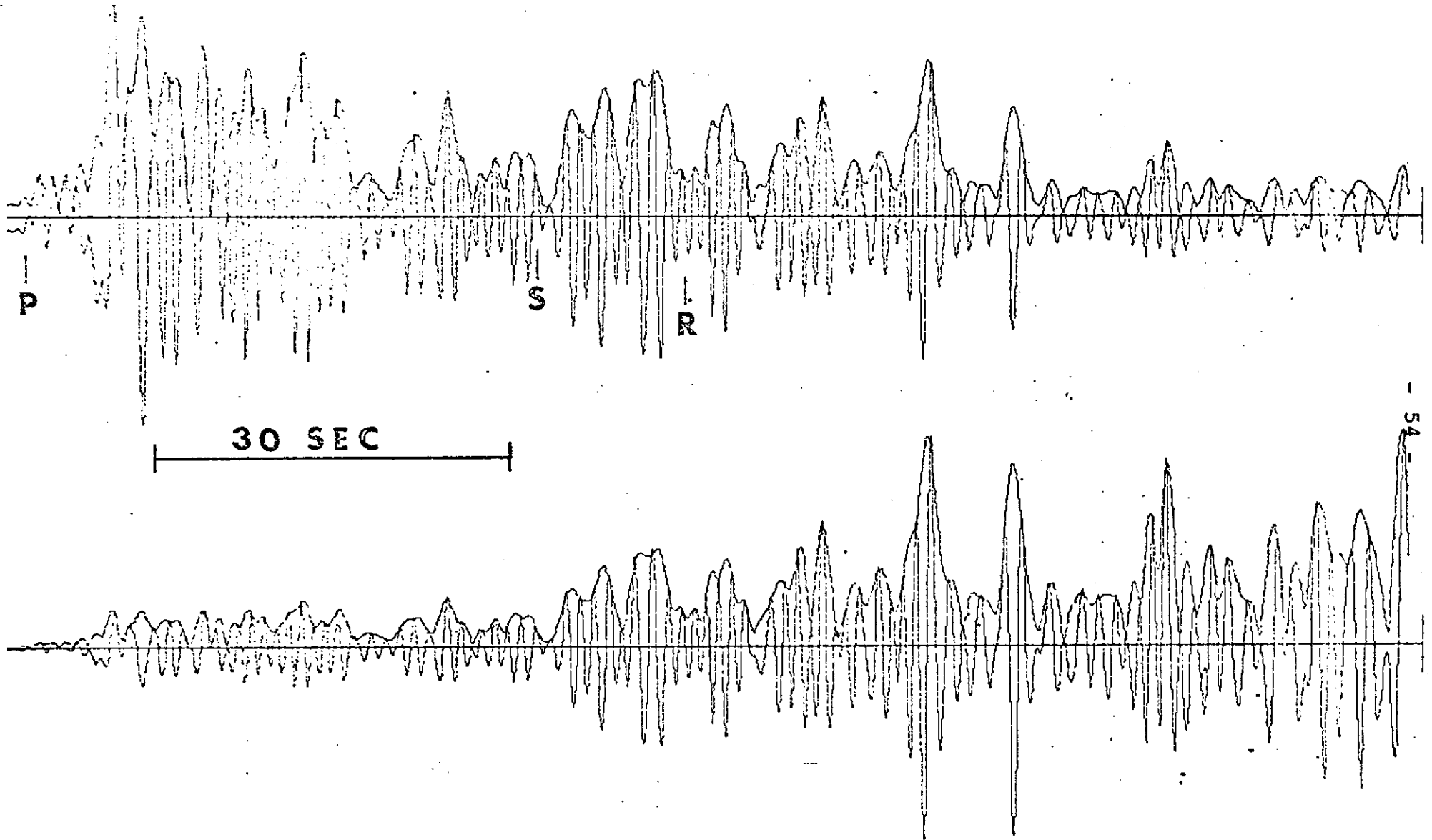


Figure 6.

APPENDIX A

Titles and Abstracts of Published Papers

Latham, G., M. Ewing, F. Press, G. Sutton (1969). The Apollo Passive Seismic Experiment. Science, 165, 241.

NO ABSTRACT.

Latham, G., M. Ewing, F. Press, G. Sutton, J. Dorman, Y. Nakamura, N. Toksöz, R. Wiggins, J. Derr, F. Duennebier (1969). Passive Seismic Experiment, Apollo 11 Preliminary Science Report, NASA SP-214, 143

NO ABSTRACT.

Latham, G., M. Ewing, F. Press, G. Sutton, J. Dorman, Y. Nakamura, N. Toksöz, R. Wiggins, J. Derr, F. Duennebier (1970). Apollo 11 Passive Seismic Experiment, Science, 167, 455.

ABSTRACT. Seismometer operation for 21 days at Tranquility Base revealed, among strong signals produced by the Apollo 11 lunar module descent stage, a small proportion of probable natural seismic signals. The latter are long-duration, emergent oscillations which lack the discrete phases and coherence of earthquake signals. From similarity with the

impact signal of the Apollo 12 ascent stage, they are thought to be produced by meteoroid impacts or shallow moonquakes. This signal character may imply transmission with high Q and intense wave scattering, conditions which are mutually exclusive on earth. Natural background noise is very much smaller than on earth, and lunar tectonism may be very low.

Latham, G., M. Ewing, F. Press, G. Sutton, J. Dorman,
Y. Nakamura, N. Toksöz, R. Wiggins, J. Derr,
F. Duennebier (1970). Apollo 11 Passive Seismic
Experiment. Proc. Apollo 11 Lunar Sci. Conf., Vol. 3,
Geochim. Cosmochim. Acta. (Suppl. 1), 2, 2309.
Pergamon.

ABSTRACT. Seismometer operation for 21 days at Tranquillity Base revealed, among strong signals produced by the lunar module (LM) descent stage, a small proportion of probable seismic signals. By similarity with the impact signal of the Apollo 12 ascent stage, they are thought to be produced by meteoroid impacts or shallow moonquakes. This signal character may imply transmission with very high Q and intense wave scattering, conditions which are mutually exclusive on earth. Natural background noise is very much smaller than on earth, and lunar tectonism may be very low.

Latham, G., M. Ewing, F. Press, G. Sutton, J. Dorman,
Y. Nakamura, N. Toksöz, R. Wiggins, R. Kovach (1970).
Passive Seismic Experiment, Apollo 12 Preliminary
Science Report, NASA SP-235, 39.

NO ABSTRACT.

Latham, G., M. Ewing, F. Press, G. Sutton, J. Dorman,
Y. Nakamura, N. Toksöz, R. Meissner, F. Duennebier,
R. Kovach, M. Yates (1970). Seismic Data from Man-
Made Impacts on the Moon, Science, 170, 620.

ABSTRACT. Unusually long reverberations were recorded from two lunar impacts by a seismic station installed on the lunar surface by the Apollo 12 astronauts. Seismic data from these impacts suggest that the lunar mare in the region of the Apollo 12 landing site consists of material with very low seismic velocities near the surface, with velocity increasing with depth to 5 or 6 kilometers per second (for compressional waves) at a depth of 20 kilometers. Absorption of seismic waves in this structure is extremely low relative to typical continental crustal materials on earth. It is unlikely that a major boundary similar to the crust-mantle interface on earth exists in the outer 20 kilometers of the moon. A combination of dispersion and scattering of surface waves probably explains the lunar seismic reverberation. Scattering of these waves implies the presence of heterogeneity within the outer zone of the

mare on a scale of from several hundred meters (or less) to several kilometers. Seismic signals from 160 events of natural origin have been recorded during the first 7 months of operation of the Apollo 12 seismic station. At least 26 of the natural events are small moonquakes. Many of the natural events are thought to be meteoroid impacts.

Latham, G., M. Ewing, F. Press, G. Sutton, J. Dorman, Y. Nakamura, N. Toksöz, F. Duennebier, D. Lammlein (1971). Passive Seismic Experiment, Apollo 14 Preliminary Science Report, NASA SP-272, 133.

NO ABSTRACT.

Latham, G., M. Ewing, J. Dorman, D. Lammlein, F. Press, N. Toksöz, G. Sutton, F. Duennebier, Y. Nakamura (1971). Moonquakes, Science, 174, 687.

ABSTRACT. Although the average rate of seismic energy release within the moon appears to be far below that of the earth, over 100 events believed to be moonquakes have been recorded by the two seismic stations installed on the lunar surface during Apollo missions 12 and 14. With few exceptions, the moonquakes occur at monthly intervals near times of perigee and apogee and show correlations with the longer-term (7-month) lunar gravity variations. The repeating moonquakes are believed to occur at not less than 10

different locations. However, a single focal zone accounts for 80 percent of the total seismic energy detected. This active zone appears to be 600 kilometers south-southwest of the Apollo 12 and 14 sites and deep within the moon. Each focal zone must be small (less than 10 kilometers in linear dimension) and fixed in location over a 14-month period. Cumulative strain at each location is inferred. Thus, the moonquakes appear to be releasing internal strain of unknown origin, the release being triggered by tidal stresses.

Wiggins, R. (1972). The General Linear Inverse Problem: Implication of Surface Waves and Free Oscillations for Earth Structure, Rev. Geophys. Space Phys., 10, 251.

ABSTRACT. The discrete general linear inverse problem reduces to a set of m equations in n unknowns. There is generally no unique solution, but we can find k linear combinations of parameters for which restraints are determined. The parameter combinations are given by the eigenvectors of the coefficient matrix. The number k is determined by the ratio of the standard deviations of the observations to the allowable standard deviations in the resulting solution. Various linear combinations of the eigenvectors can be used to determine parameter resolution and information distribution among the observations. Thus, we can determine where information comes from among the observations and exactly

how it constrains the set of possible models. The application of such analyses to surface-wave and free-oscillation observations indicates that (1) phase, group, and amplitude observations for any particular mode provide basically the same type of information about the model; (2) observations of overtones can enhance the resolution considerably; (3) the degree of resolution has generally been overestimated for many model determinations made from surface waves; and (4) computation of parameter and information resolution is such a simple extension of any inversion procedure based on perturbation parameters that such inversion studies are incomplete without considering resolution.

Toksoz, M. N., F. Press, K. Anderson, A. Dainty, G. Latham, M. Ewing, J. Dorman, D. Lammlein, G. Sutton, F. Duenebier, Y. Nakamura (1972). Lunar Crust: Structure and Composition, Science, 176, 1012.

ABSTRACT. Lunar seismic data from artificial impacts and three Apollo seismometers are interpreted to determine the structure of the moon's interior to a depth of about 100 km. In the Fra Mauro region of Oceanus Procellarum, the moon has a 65 km thick layered crust. Other features are: i) the upper layer velocities are consistent with those of lunar basalts to a depth of 25 km; ii) between 25 and 65 km depth, nearly constant velocity (6.8 km/sec) corresponds to those of gabbroic and anorthositic rocks;

iii) the apparent velocity is very high (about 9 km/sec) in the lunar mantle immediately below the crust.

Toksoz, M. N., F. Press, K. Anderson, A. Dainty, G. Latham, M. Ewing, J. Dorman, D. Lammlein, G. Sutton, F. Duennebier, Y. Nakamura (1972). Velocity Structure and Properties of the Lunar Crust, The Moon, in press.

ABSTRACT. Lunar seismic data from three Apollo seismometers are interpreted to determine the structure of the moon's interior to a depth of about 100 km. The travel times and amplitudes of P arrivals from Saturn IV B and LM impacts are interpreted in terms of a compressional velocity profile. The most outstanding feature of the model is that, in the Fra Mauro region of Oceanus Procellarum, the moon has a 65 km thick layered crust. Other features of the model are: i) rapid increase of velocity near the surface due to pressure effects on dry rocks, ii) a discontinuity at a depth of about 25 km, iii) near constant velocity (6.8 km/sec) between 25 and 65 km deep, iv) a major discontinuity at 65 km marking the base of the lunar crust, and v) very high velocity (about 9 km/sec) in the lunar mantle below the crust. Velocities in the upper layer of the crust match those of lunar basalts while those in the lower layer fall in the range of terrestrial gabbroic and anorthositic rocks.

Toksöz, M. N., F. Press, A. Dainty, K. Anderson, G. Latham, M. Ewing, J. Dorman, D. Lammlein, G. Sutton, F. Duennebier (1972). Structure, Composition, and Properties of Lunar Crust, Proc. Third Lunar Sci. Conf., in press.

ABSTRACT. Lunar seismic data from three Apollo seismometers are interpreted to determine the structure of the moon's interior to a depth of about 100 km. The travel-times and amplitudes of P and S arrivals from Saturn IV-B and LM impacts are interpreted in terms of a velocity profile. The most outstanding feature of the model is that, in the Fra Mauro region of Oceanus Procellarum, the moon has a 65 km-thick layered crust. Other features of the model are: i) rapid increase of velocity near the surface due to pressure effects on dry rocks, ii) a discontinuity at a depth of about 25 km, iii) near-constant velocities between 25 and 65 km deep, iv) a major discontinuity at 65 km marking the base of the lunar crust, and v) very high apparent-velocities (about 9 km/sec for P waves) in the lunar mantle below the crust. Velocities in the upper layer of the crust match those of lunar basalts while those in the lower layer fall in the range of terrestrial gabbroic and anorthositic rocks. The high apparent velocities in the mantle, if they persist, imply a differentiated lunar mantle whose composition varies with depth.

APPENDIX B

List of Oral Presentations

- Latham, G., M. Ewing, F. Press, G. Sutton . The Apollo Lunar Seismic Experiment. Fall Meeting, Amer. Geophys. Un., Nov. 1969, San Francisco.
- Latham, G., M. Ewing, F. Press, G. Sutton, J. Dorman, Y. Nakamura, M. N. Toksöz, R. Wiggins, J. Derr, F. Duennebier. Apollo 11 Passive Seismic Experiment. Apollo 11 Lunar Sci. Conf., Jan. 1970, Houston.
- Latham, G., M. Ewing, J. Dorman, F. Press, M. N. Toksöz, R. Wiggins, G. Sutton, Y. Nakamura, R. Kovach. Results from the Apollo Passive Seismic Experiment. Spring Meeting, Amer. Geophys. Un., April 1970, Washington D.C.
- Latham, G., M. N. Toksöz, F. Press, K. Anderson, M. Ewing, J. Dorman, D. Lammlein, G. Sutton, F. Duennebier, Y. Nakamura. Moonquakes and Lunar Tectonism, Lunar Sci. Inst. Conf. on Lunar Geophys., Oct. 1971, Houston.
- Toksoz, M. N., F. Press, K. Anderson, G. Latham, M. Ewing, J. Dorman, D. Lammlein, G. Sutton, F. Duennebier, Y. Nakamura. Artificial Impacts and Internal Structure of the Moon. Lunar Sci. Inst. Conf. on Lunar Geophys., Oct. 1971, Houston.
- Latham, G., M. Ewing, J. Dorman, D. Lammlein, F. Press, M. N. Toksöz, Y. Nakamura, G. Sutton, F. Duennebier. Moonquakes. Fall Meeting, Amer. Geophys. Un., Nov. 1971, San Francisco.

Toksöz, M. N., F. Press, K. Anderson, G. Latham, M. Ewing,
J. Dorman, D. Lammlein, G. Sutton, F. Duennebier,
Y. Nakamura. Internal Structure of the Moon. Fall
Meeting, Amer. Geophys. Un., Nov. 1971, San Francisco.

Latham, G., M. Ewing, F. Press, G. Sutton, J. Dorman,
Y. Nakamura, M. N. Toksöz, D. Lammlein, F. Duennebier.
Moonquakes and Lunar Tectonism - Results from the
Apollo Passive Seismic Experiment. Third Lunar
Sci. Conf., Jan. 1972, Houston.

Toksöz, M. N., F. Press, K. Anderson, A. Dainty, G. Latham,
M. Ewing, J. Dorman, D. Lammlein, G. Sutton, F. Duennebier,
Y. Nakamura. Velocity Structure and Properties of
the Lunar Crust. Third Lunar Sci. Conf., Jan. 1972,
Houston.

Duennebier, F., G. Sutton, G. Latham, M. Ewing, J. Dorman,
D. Lammlein, F. Press, M.N. Toksöz, Y. Nakamura.
Moonquakes Recorded by the Apollo Short-Period Seis-
mometers. Annual Meet., Seis. Soc. Amer., March
1972, Honolulu.

Dainty, A. M., K. R. Anderson. Seismic Scattering in the
Moon and the Earth. Spring Meeting, Amer. Geophys. Un.,
April 1972, Washington D.C.

Dorman, J., G. Latham, M. Ewing, D. Lammlein, F. Press,
M. N. Toksöz, G. Sutton, F. Duennebier, Y. Nakamura.
Seismic Observation of Meteoroid Impacts on the Moon.
Spring Meeting, Amer. Geophys. Un., April 1972, Washington
D.C.